BUDAPEST UNIVERSITY OF TECHNOLOGY AND ECONOMICS
Faculty of Mechanical Engineering
Department of Applied Mechanics

Dynamics of rolling of railway wheelsets

DIPLOMA THESIS

Author:

Máté Antali
mechanical engineering modelling MSc student

Supervisors:

Prof. Gábor Stépán
Budapest University of Technology and Economics
Department of Applied Mechanics

Prof. John Hogan
University of Bristol
Department of Engineering Mathematics

Budapest, 2012 a. D.

Every man naturally desires knowledge,
but what good is knowledge without fear of God?
The more you know and the better you understand,
the more severely will you be judged,
unless your life is also the more holy.
Do not be proud, therefore, because of your learning or skill,
but fear because of the knowledge given you.

/Thomas a Kempis: The Imitation of Christ/

Contents

Introduction

Most of us must have travelled thousands of kilometres by train, but it is not a usual activity to stare the wheels of a railway vehicle from a short distance. If we still try, we can observe that the wheels are not exactly cylindrical, but slightly conical. This little difference in the geometry let us to produce wheelsets – pairs of wheels – without a differential gear, and it provides a very effective way to follow the curves of the track.

Conical shape of wheels is certainly one of the most ingenious ideas from the history of railways, but it has a side-effect which usually called *hunting*. This phenomenon covers a type of vibration of the wheelset, which can reach the vehicle or can be a reason of derailment. Therefore hunting motion is a subject or research for a very long time.

Nowadays complicated contact mechanical models are used to describe and understand hunting motion, aspects like elastic deformation, friction or plastic effects are often included into them. Most of them are built on the top of a linear rigid-body motion, where the angle of the cone and the change of the orientation are assumed to be small. Models containing the full three-dimensional description seem to be unavailable in the literature, even for the simple one-point rolling.

In this diploma thesis the task is to create a mechanical model to investigate the geometric nonlinearities of three-dimensional motion during hunting of railway wheelsets. Rigid bodies are considered with one-point rolling, but calculations are performed without the usual linear approximations. After deriving the equations of motions we will try to explore its dynamics by using various methods.

Chapter 1

Phenomenon and modelling

1.1 Phenomenon of hunting motion

First of all the important notions and concepts are presented in connection with the hunting phenomenon of railway wheelsets. For a more detailed introduction see for the railway dynamics handbooks of Wickens [17] or Iwnicki [5].

1.1.1 Wheelsets and vehicle

In the case of railway vehicles we usually speak about wheelsets instead of wheels, because a pair of wheels is produced and used as a single part. Sketch of a typical wheelset can be seen in Figure 1.1. The conical wheel threads provide the rolling connection between the rails and the wheelset, the flanges secure the wheelset against derailment and the axle connects the wheels rigidly with each other and possibly with the engine or the generator of the vehicle.

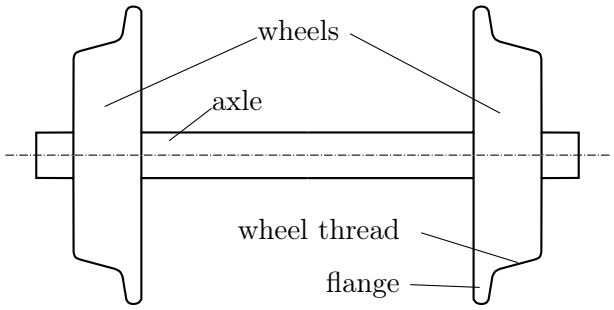

Figure 1.1: Elements of a wheelset

It can be determined from the degrees of freedom, that rigid connection between

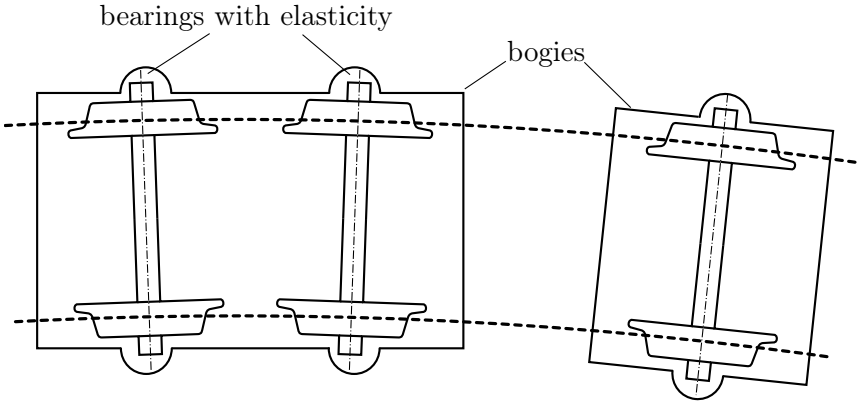

Figure 1.2: Schematic arrangements of bogies. If there is only one wheelset (right), it is enough in each bearing to ensure an elastic radial foundation in two dimensions, which can be created typically by springs. If there is two wheelsets in the bogie (left), then between them also the relative rotation in the horizontal plane is to be allowed, which leads to complicated constructions in practice.

the bearings of more wheelsets makes the system over-constrained, and it disables the possibility of proper rolling of the wheelsets. Therefore bearings of wheelsets are suspended to bogies, which can rotate freely around vertical axes relative to the body of the vehicle. Usually more than one wheelset can be connected to one bogie. In both cases the bearings can be constructed to ensure the independent three-dimensional motion of all wheelsets in order to prevent large-scale sliding. These arrangements can be seen in Figure 1.2.

1.1.2 Guidance and lateral displacement

From the very beginning of railway history, the wheel threads are not cylindrical- but slightly conical-shaped where the radius decreases outwards. This geometry is crucial for the proper operation of wheels through allowing a small change in the radius of the wheels. On one hand, this ability substitutes the differential gear, on the other hand, it provides the guidance from the changing curvature of the rails and keeps the wheelset on the track.

The differential mechanism can be seen in Figure 1.3. On a straight track the wheelset is located symmetrically related to the rails, the radii of rolling are the same. In a curved track the wheelset moves a bit outwards, which reduces the inner and increases the outer radius of rolling. This lateral displacement enables both wheels to roll in curves. Curvature of the track is designed to change continu-

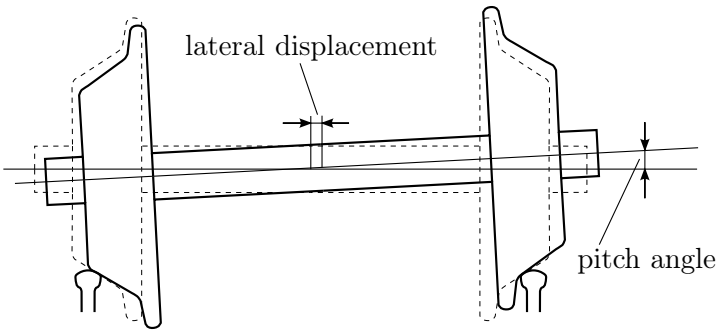

Figure 1.3: Behaviour of a wheelset in a curve. The wheelset ‚slides' outwars with the amount of the lateral displacement which increases the outer radius and creates the pitch angle. Pitch angle is always smaller than the angle of the cone.

ously, therefore change in the lateral displacement can tune the radii of the wheels smoothly to the shape of the track. Lateral displacement appears together with a rotation of the axis, which is called the *pitch angle*.

Even more important, that the conical shape can itself produce a resultant contact force which makes the wheelset to follow the track, even without using the flanges. During ordinary operation, the flanges do not touch the rails. However if vibrations or sliding suddenly create a large lateral displacement, impact between the flange and the rail can prevent derailment of the wheelset.

1.1.3 Natural motion and hunting motion

From the previous subsection we can conclude, that if the curvature of the track is constant, there exists a lateral motion which can create a *natural motion* of the wheelset. That is, in the co-moving reference frame of the vehicle the symmetry axis of the wheelset does not move, and the motion of the wheelset is a pure rotation around this axis.

However this natural motion can be disturbed due to different circumstances (for example sliding, impacts, etc.), and a so-called *hunting motion* can occur. This is an oscillation superposed on the natural motion, which contains continuous change in the lateral displacement and in the orientation of the symmetry axis of the wheelset.

This motion, also called *parasite motion* can be understood from Figure 1.4. Together with the lateral displacement the so-called *yaw angle* is changing, which measures the horizontal rotation of the wheelset. Hunting motion can be a periodic

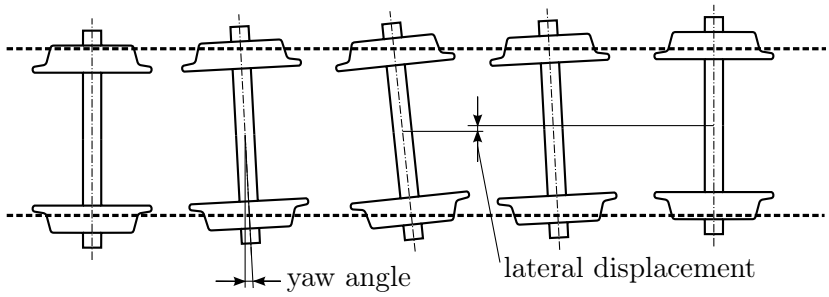

Figure 1.4: Sketch of hunting motion. Zero value of yaw angle corresponds to local maximum of lateral displacement and it becomes maximal where lateral displacement vanishes. This creates a vibration, which is generally non-periodic according to the experiences. Yaw angle can be much larger than the angle of the cone.

motion, but it can also intensify or die down. From engineering point of view, hunting motion is not favourable because it can cause unwanted vibrations of the vehicle and it increases the dynamic loads of the parts especially near the contact. In more serious case hunting motion can produce so large vibrations which can cause derailment of the wheelset.

Therefore it is important to minimize hunting motion by finding the conditions for increasing or decreasing the intensity of hunting. However lots of circumstances can modify this motion, and it usually complicated to build an appropriate model.

1.2 Models in the literature

Let us now make a short overview of the existing mechanical models of hunting motion. For a more detailed overview see for the contact mechanics books of Johnson [7], or Kalker [10], the railway dynamics textbook of Wickens [17] or the historical overview of Knothe [12].

Models of hunting motion can be classified according to different aspects. A single wheelset or more wheelsets in a bogie can be investigated as well as a whole vehicle. The vehicle can have a constant or a changing velocity, and the track can be straight or curved.

In this project we restrict the analysis to a single wheelset moving on a straight track with a constant velocity. The wheelsets and bodies can be assumed simply either rigid or elastic bodies. Another possibility is to consider elasticity only in the region of the contact. Of course different assumptions can be used for the wheelset and for the wheels. Now some of the important models are introduced.

1.2.1 Rigid models

Both the wheelset and the rails can be considered as rigid bodies. Then the contact of the bodies can be described by their outer surfaces, which are often assumed to be smooth. In the case of two general rigid surfaces they touch each other at a single point, which is called the *contact point*, and the model is called the *one-point contact model*. At the contact point the tangent planes of the surfaces coincide.

One-point can exit continuously in time only if the normal component of the relative velocity at the contact point is zero ($\mathbf{v}_n = \mathbf{0}$). The tangential component of the relative velocity in the contact point ($\mathbf{v}_t$) is called the *velocity of sliding*. The vector of the relative angular velocity can be also divided into tangential ($\boldsymbol{\omega}_t$) and normal ($\boldsymbol{\omega}_n$) component, they are called *angular velocity of rolling* and *angular velocity of spinning*, respectively. The one-point contact restricts only one degree-of-freedom from the motion, the possible velocities can be described by $\boldsymbol{\omega}_t, \boldsymbol{\omega}_n$ and $\mathbf{v}_t$.

Usually we call rolling the case where $\mathbf{v}_t = \mathbf{0}$, in other words when the relative velocity at the contact point is zero. If $\mathbf{v}_t$ is non-zero, the motion is called sliding.

From the analysis of the degrees of freedom of a single wheelset with one-point contact and rolling on each wheel, it turns out, that if the velocity of the vehicle is given, then the motion of the wheelset can be determined purely from kinematics. The first approximate calculation was done in 1883 by Klingel [11]. For very small value of the angle of the cone (denoted by α) he derived the following linear approximation of the equation of motion expressed by the lateral displacement y:

$$\frac{\mathrm{d}^2 y}{\mathrm{d}t^2} + v^2 \frac{h}{\hat{d}\hat{R}} y = 0, \tag{1.2.1}$$

from which a pure sinusoidal solution $y(t) = \sin(\omega_K t)$ occurs with the angular frequency

$$\omega_K := v\sqrt{\frac{h}{\hat{d}\hat{R}}} \tag{1.2.2}$$

Here $\hat{d}$ denotes the half-distance between the contact points, and $\hat{R}$ is the radius of rolling, both corresponding to the natural motion. The tangent of the cone is denoted by $h = \tan\alpha$ and v is the velocity of the vehicle. These quantities can be found in Figure 1.5. Expression (1.2.2) is called *Klingel's formula*, and it can be found in every railway dynamics books. In fact for small α and y values it is accurate enough for engineering practice, especially if we consider the limits of the

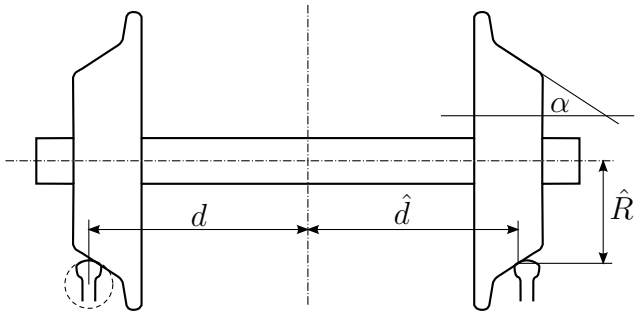

Figure 1.5: Important parameters of a wheelset. The half-distance $\hat{d}$ is measured between the contact points in natural position, and d is the half-distance of the centres of the approximate cylinders of the rail profile. If α is small, then they are close to each other.

one-point contact model. From (1.2.1) a similar equation can be obtained for the yaw angle, while the effect of the pitch angle is neglected in this investigation.

A correction of this model was made in 1993 by Gábor Lóránt [13], which is valid also for large α angle, and the following formulae was derived for the hunting angular frequency:

$$\omega_L := v\sqrt{\frac{hd}{\hat{d}^2\hat{R}}} = \omega_K\sqrt{\frac{d}{\hat{d}}} \tag{1.2.3}$$

Here the rails are considered to be cylinders and d denotes the half-distance between the axes of these cylinders.

1.2.2 Elastic models

The rails and the wheelset can also be considered as elastic bodies. Then we can use the tool kit of continuum mechanics in the model to describe the stress, strain and displacement fields of the bodies. For the modelling of the material of the wheelset and the rails, simple material models can be used. The boundary conditions are not obvious both between the wheelset and the vehicle, both at the foundation of the rails.

In the case of elastic bodies a finite contact surface appears instead of a single contact point (Figure 1.6). Points of the contact surface have zero normal velocity and can have two possible states, *micro-slip* and *micro-stick*, according to their tangential velocities. Points in the stick state have zero tangential velocity, and tangential velocity of points in slip state is non-zero. As velocity changes continuously, the contact surface consists of finite slip and stick zones.

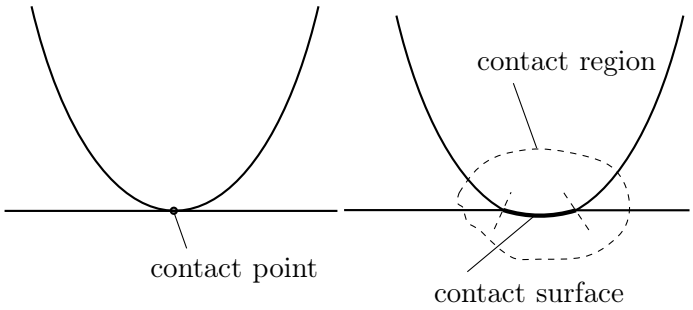

Figure 1.6: Difference between rigid and elastic contact. The common part of the surfaces is called the contact surface. A common-used approximation restricts the elastic effect into a practically chosen contact region.

The complexity of the problem causes that apart from semi-empirical and approximate methods, the hunting motion can be examined only by numerical methods like finite element analysis. Due to the contact analysis and the transient effects from the hunting, it is a complicated task to get accurate results even with a professional FEA software. There are no widespread models used typically for hunting motion, usually the combination of general-purpose FEA algorithms are used in practice.

1.2.3 Combined rigid-elastic models

The main idea of most widely-used contact models, that the elastic deformation is taken into consideration only in the *contact region*, in the vicinity of the contact surface, as illustrated in Figure 1.6. If the contact forces are not too large compared to the stiffness of the bodies, then the contact surface is small, stresses and strains near the contact surface are much larger than in other parts of the bodies. The contact region is an appropriately chosen volume around the contact surface, which includes points of large strains. Therefore elastic models can be used in the contact region, but globally the bodies can be considered rigid.

The localised elastic assumption has the advantage that contact problems with different global geometries can be investigated together if the behaviour in the contact surface is similar. The first fundamental theory was created in 1882 by Hertz [3]. He investigated the strain and stress fields at contact regions between bodies approximated locally by plane-, cylinder- and sphere-shaped geometry. Hertz's theory became the basis of contact mechanics, and in the next decades it was extended

and generalized by many researchers.

The problem from the rigid body approach was investigated by Reynolds [15], who performed experiments of rolling bodies made of different materials. He experienced the phenomenon of creep, that means a rigid motion very close to rolling, but a small amount of sliding seems to appear. The notion of *creep velocity* is used for measuring the slight sliding of the surfaces. The *creep ratio* is defined as

$$\nu_c = \frac{\mathbf{v}_t}{V} \tag{1.2.4}$$

where V is the speed of rolling, which is the speed of translation of the contact point on the surfaces, which can be calculated from $\boldsymbol{\omega}_t$ and the curvature of the surfaces. A similar coefficient can be defined also for spinning. If $\nu_c = 0$ then the ideal rolling is obtained, but for real rolling ν_c is a small but finite number due to deformations and slip. It is determined by the forces in the contact region, from which the tangential forces are called creep forces. Creep models creates the connection between the creep force and the creep ratio.

Already Hertz noticed the importance of the contact theory specifically for the dynamics of railway wheelsets, but the first successful application of Hertz's Theory for the creep of the hunting motion was made in 1926 by Carter [1]. He was able to calculate the critical speed of the vehicle, above which the hunting motion becomes unstable. The same result was presented independently by four other authors ([7], p. 252) within a few years.

Although the main concept remained the same, these results were developing together with the new results of the general contact mechanics. With the works of Johnson [6] and Kalker [9] plastic behaviour, nonlinear creep theory and friction forces were introduced to the models as well as exploring the micro-slip and micro-stick regions of the contact surface. Theories used nowadays are mainly based on these results supported by computer techniques.

1.3 Aim of this thesis

In the present work the rigid assumption is going to be used do explore the nonlinear effects caused by the three-dimensional rolling of the conical wheelsets. Most of dynamic calculations of hunting, from Klingel's equation (1.2.1) to the modern models use the assumption, that the cone angle α is very small. As for practically-used geometries α is a few degrees, this assumption works nicely..

However analysis of hunting motion with one-point rolling model can be useful, even if most creep models calculate the small deviation from it. From a three-dimensional nonlinear model the full scope of the rigid model can be separated from the elastic effects. As it was mentioned, Lóránt made a full three-dimensional calculation of the problem, however the formulae became impracticably long. Although he succeeded to obtain the linear formula for the hunting frequency, he did not get an explicit formula for the differential equation of the system. The stability of the natural motion of the rigid model is still an open question.

This project is supposed to answer some of these problems.

Chapter 2

Mechanical model

2.1 Physical description

A single railway wheelset is investigated travelling along a straight track. Our objective is to build up the simplest mechanical model which is able to describe the phenomenon of hunting motion, but already contains the nonlinearities caused by three-dimensional motion.

2.1.1 Model of the track

The rails are modelled as rigid bodies, and their geometry is approximated by two parallel cylinders, because top of most common-used rail profiles is described by a single arc. If the contact points remain on this arc, and do not reach the fillets of the edges, then approximating with cylinders does not mean any difference compared to the full profile. Let the radius be denoted by r.

The foundation of the wheels are also assumed to be rigid, thus the rails are modelled to be fixed to an inertial frame. Let the axes of the cylinders lay in the same horizontal plane and let the distance of the axes be $2d$. The sketch of the geometry can be seen in Figure 2.1.

2.1.2 Model of the wheelset

The wheelset is also considered to be rigid. From the wheel profile neither the flanges, nor the transitional curves but only the conical wheel thread is modelled. Therefore the geometry of the wheelset can be considered as a so-called bicone, two

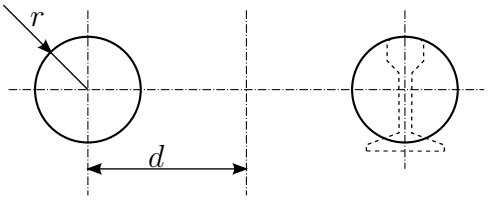

Figure 2.1: Model of the track. The modelled arc of the rail profile typically has a radius r of a few hundreds of millimetres and an opening angle of 5-10 degrees. The notation of d is consistent with Figure 1.5, its value is typically around 1500 mm.

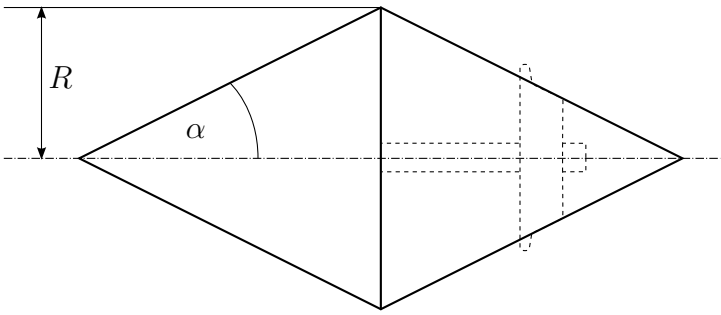

Figure 2.2: Model of the wheelset. R is not the same as $\hat{R}$ in Figure 1.5, but at small α they are almost equal. Typical value of α is 1-5 degrees.

identical right circular cones glued together at their base circles. Let the bottom radius be R and the half of the opening angle is α.

The mass and the mass moments of inertia are not defined because they are not needed for the following calculations..

2.1.3 Contact and loads

The rigid property is assumed in the whole body, therefore one-point contact model is used between the wheelset and the rails. There must be a contact point between each half of the bicone and the corresponding rail. At the contact points the surfaces must be tangential to each other.

Ideal rolling is supposed, therefore in the contact points relative tangential velocities between the surfaces must be zero. As the rails are fixed, velocity of the bicone at the contact points can be prescribed to be zero.

It is assumed, that the constant velocity v of the vehicle is not modified by the motion of the wheelset. The connection between the bearings and the vehicle is supposed to be elastic, which would result a complicated boundary condition.

However it is a reasonable assumption that the centre of the wheelset has also a constant velocity component v to the direction of the track.

The forces acting on the wheelset without driving, can arise from four sources: from the gravity, from the contact, from the bearings and from the driving. We will see later that the rolling constraints and the pulling with constant velocity determine the equations of the system without knowing the forces. Therefore the modelling of the forces is not necessary.

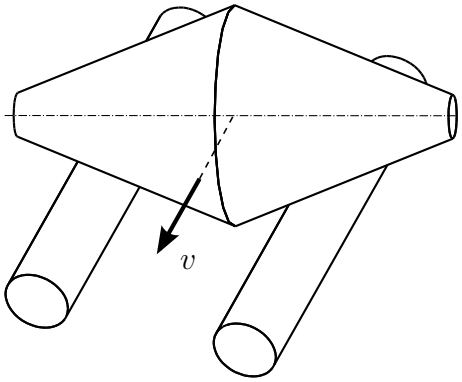

Figure 2.3: Towing load of the wheelset. v denotes only the component parallel to the track. The another two components of velocity of the geometric centre is allowed to change freely.

2.2 Mathematical implementation

In this section the physical requirements of our mechanical model are implemented in mathematical model. During the calculations $:=$ means the defining equation of an object, $\hat{=}$ denotes an axiom of the model, and the single $=$ means an equality derived from existing equations.

2.2.1 Notations

The motion of the wheelset is described in a three-dimensional vector space $\mathbb{V}$, the vectors are denoted by small boldface letters, like $\mathbf{v} \in \mathbb{V}$. A scalar product

$$(\mathbb{V}, \mathbb{V}) \to \mathbb{R}, \quad (\mathbf{v}, \mathbf{w}) \to \mathbf{v} \cdot \mathbf{w} \tag{2.2.1}$$

and a vector product

$$(\mathbb{V}, \mathbb{V}) \to \mathbb{V}, \quad (\mathbf{v}, \mathbf{w}) \to \mathbf{v} \times \mathbf{w} \tag{2.2.2}$$

are defined on $\mathbb{V}$.

The dual space of $\mathbb{V}$, is denoted by $\mathbb{V}^* = \mathrm{Hom}(\mathbb{V}, \mathbb{R})$. The dual vector of a vector $\mathbf{v}$, is denoted by $\mathbf{v}^* \in \mathbb{V}^*$ which satisfies equation

$$\mathbf{v}^* \mathbf{w} = \mathbf{v} \cdot \mathbf{w} \tag{2.2.3}$$

for all $\mathbf{w} \in \mathbb{V}$.

The linear transformations of $\mathbb{V}$ are denoted by capital boldface letters, $\mathbf{A} \in \mathrm{Hom}(\mathbb{V}, \mathbb{V})$. The inverse of $\mathbf{A}$ is denoted by $\mathbf{A}^{-1} \in \mathrm{Hom}(\mathbb{V}, \mathbb{V})$, for which

$$\mathbf{A}\mathbf{A}^{-1} = \mathbf{A}^{-1}\mathbf{A} = \mathbf{I}, \tag{2.2.4}$$

and $\mathbf{I}$ is the identity transformation.

The set of orthonormal, dextrorotatory bases on $\mathbb{V}$ is denoted by $\mathrm{Bas}(\mathbb{V}) \subset \mathbb{V}^3$. A basis as a triplet of vectors, denoted by $(\mathbf{b}_i) \in \mathrm{Bas}(\mathbb{V})$ where $i \in \{1, 2, 3\}$. Orthonormal and dextrorotatory properties mean

$$\mathbf{b}_i \cdot \mathbf{b}_j = \delta_{ij} \tag{2.2.5}$$

and

$$\mathbf{b}_i \times \mathbf{b}_j = \epsilon_{ijk} \mathbf{b}_k \tag{2.2.6}$$

for all $i, j, k \in \{1, 2, 3\}$. Here δ_{ij} is the Kronecker-symbol and ϵ_{ijk} the Levi-Civita symbol. For the indices Einstein's summation notation convention is used here and during the following calculations of this chapter. For the details see for the first chapter of [4].

Coordinates of a vector $\mathbf{v}$ with respect to a basis $\mathbf{b}_i$ are denoted by

$$v_i = \mathbf{b}_i^* \mathbf{v} \tag{2.2.7}$$

Components of a linear transformation $\mathbf{A}$ is denoted similarly, by

$$A_{ij} = \mathbf{b}_i^* \mathbf{A} \mathbf{b}_j \tag{2.2.8}$$

These coordinates of vectors and transformations are enumerated in column matrices and square matrices, respectively.

A linear transformation $\mathbf{T}$ is called a rotation if for any basis $(\mathbf{b}_i) \in \mathrm{Bas}(\mathbb{V})$, the transformed triplet is also an orthonormal, dextrorotatory basis, that is:

$$(\mathbf{T}\mathbf{b}_i) \in \mathrm{Bas}(\mathbb{V}) \tag{2.2.9}$$

The set of rotations are denoted by $\mathrm{Rot}(\mathbb{V}) \subset \mathrm{Hom}(\mathbb{V}, \mathbb{V})$.

2.2.2 Free motion of the wheelset

The geometry of the wheelset is given in its material reference frame. This coordinate system is moving, therefore its motion is to be described first.

Let us consider a transformation of a general rigid body motion, denoted by $\mathbf{u} : \mathbb{V} \to \mathbb{V}$, which can be composed from a translation and a rotation:

$$\mathbf{u}(\mathbf{r}) := \mathbf{R}\mathbf{r} + \mathbf{x}, \tag{2.2.10}$$

where $\mathbf{x} : \mathbb{R} \to \mathbb{V}, t \to \mathbf{x}(t)$ is the translation of a chosen pivot point and $\mathbf{R} : \mathbb{R} \to \mathrm{Rot}(\mathbb{V}), t \to \mathbf{R}(t)$ is the rotation of the body around the pivot point.

Let us differentiate (2.2.10) with respect to time. After substituting the inverse of (2.2.10) the Eulerian velocity field is obtained:

$$\mathbf{v}(\mathbf{r}) := \dot{\mathbf{u}} \circ \mathbf{u}^{-1}(\mathbf{r}) = \boldsymbol{\Omega}(\mathbf{r} - \mathbf{x}) + \dot{\mathbf{x}} \tag{2.2.11}$$

Here $\dot{\mathbf{x}}$ is the velocity of the pivot point and $\boldsymbol{\Omega} := \dot{\mathbf{R}}\mathbf{R}^{-1}$ is the angular velocity of the body in tensor form. From this point a dot over a symbol always denotes differentiation with respect to time.

These objects describe the free motion of the wheelset. The position of the body is given by the pair $(\mathbf{x}, \mathbf{R})$, and the state of velocity is described by the triplet $(\dot{\mathbf{x}}, \boldsymbol{\Omega}, \mathbf{x})$. For the calculations it is necessary to express these by scalar functions.

Let $(\mathbf{e}_i) \in \mathrm{Bas}(\mathbb{V})$ be a basis fixed to the rails, where $\mathbf{e}_1$ point to the moving direction of the vehicle and $\mathbf{e}_3$ points vertically upwards, as can be seen in Figure 2.4.

The vector $\mathbf{x}$ is simply parametrised by its Cartesian coordinates with respect to $(\mathbf{e}_i)$:

$$\mathbf{e}_i^* \mathbf{x} := \begin{bmatrix} x \\ y \\ z \end{bmatrix} \tag{2.2.12}$$

The rotation tensor $\mathbf{R}$ is parametrised with Euler angles:

$$\mathbf{e}_i^* \mathbf{R} \mathbf{e}_j := P_{ik}(\vartheta) Q_{kl}(\psi) R_{lj}(\varphi), \tag{2.2.13}$$

where

$$P_{ij}(\vartheta) := \begin{bmatrix} 1 & 0 & 0 \\ 0 & \cos\vartheta & -\sin\vartheta \\ 0 & \sin\vartheta & \cos\vartheta \end{bmatrix} \tag{2.2.14}$$

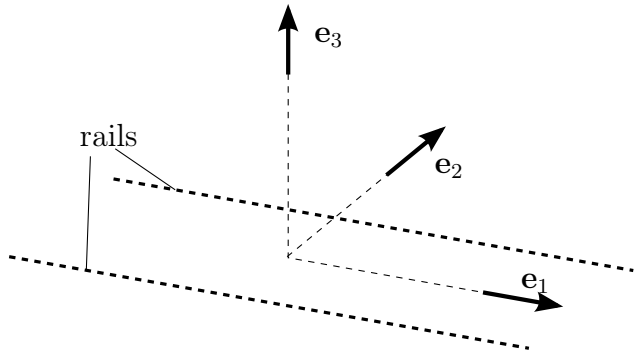

Figure 2.4: Directions of basis ($\mathbf{e}_i$) fixed to the track. $\mathbf{e}_1$ and $\mathbf{e}_2$ are in a horizontal plane, $\mathbf{e}_1$ shows the direction of the track.

$$Q_{ij}(\psi) := \begin{bmatrix} \cos\psi & -\sin\psi & 0 \\ \sin\psi & \cos\psi & 0 \\ 0 & 0 & 1 \end{bmatrix} \tag{2.2.15}$$

$$R_{ij}(\varphi) := \begin{bmatrix} \cos\varphi & 0 & \sin\varphi \\ 0 & 1 & 0 \\ -\sin\varphi & 0 & \cos\varphi \end{bmatrix} \tag{2.2.16}$$

The angles φ, ψ and ϑ are called *roll angle*, *yaw angle*, and *pitch angle*, respectively. The roll angle corresponds to the rotation of the wheelset around its symmetry axis. The pitch and yaw angles determine the direction of this symmetry axis, their meaning can be seen in Figures 2.5-2.6.

The Euler angles are chosen so, that the state $\vartheta = 0$ and $\psi = 0$ corresponds to the natural position of the wheelset. Rotations of the Euler angles define a sequence of bases which will be used in the following calculations:

$$\begin{aligned} \mathbf{f}_i &:= P_{ij}^{-1}(\vartheta)\,\mathbf{e}_j \\ \mathbf{g}_i &:= Q_{ij}^{-1}(\psi)\,\mathbf{f}_j \\ \mathbf{h}_i &:= R_{ij}^{-1}(\varphi)\,\mathbf{g}_j, \end{aligned} \tag{2.2.17}$$

where $P_{ij}^{-1}(\vartheta)$, $Q_{ij}^{-1}(\psi)$ and $R_{ij}^{-1}(\varphi)$ are the corresponding inverse matrices. Using (2.2.17) and (2.2.13) we get:

$$\mathbf{h}_i = \mathbf{R}\mathbf{e}_i, \tag{2.2.18}$$

hence the basis $\mathbf{h}_i$ is fixed to the moving wheelset.

The geometric state of the system is now expressed with six real variables, the state of the unconstrained wheelset can be described by

$$q^u := (x, y, z, \varphi, \psi, \vartheta) \in \mathbb{R}^6 \tag{2.2.19}$$

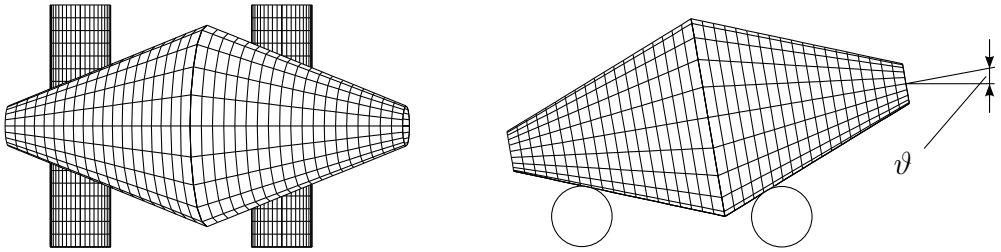

Figure 2.5: Meaning of the pitch angle, $\vartheta > 0, \psi = 0$

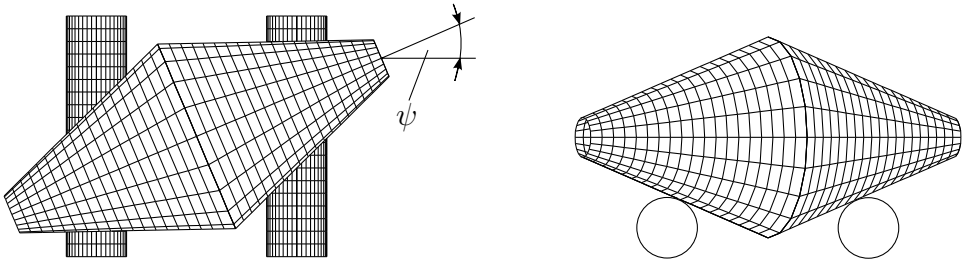

Figure 2.6: Meaning of the yaw angle, $\psi > 0, \vartheta = 0$

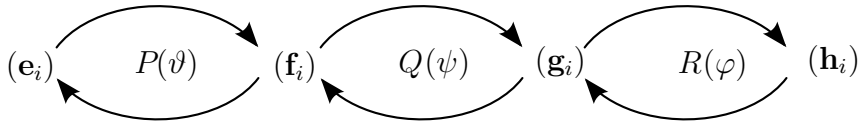

Figure 2.7: Connection between bases and Euler angles. To the direction of lower arrows the matrices can be used for basis transformation of vector components, to the direction of upper arrows the corresponding inverse is needed.

2.2.3 Geometry of the bodies

We define the rigid bodies by their surfaces described as two-parametric vector functions. The rails are modelled as two infinite parallel cylinders with radius r and distance $2d$ apart. Let $\boldsymbol{\rho}^l$ and $\boldsymbol{\rho}^r$ denote the surfaces of left and right rails. The functions of the rails are described by the fixed basis $(\mathbf{e}_i)$:

$$\mathbf{e}_i^* \boldsymbol{\rho}^{lr}(\xi, \gamma) := \begin{bmatrix} \xi \\ r \sin\gamma \pm d \\ r \cos\gamma \end{bmatrix} \tag{2.2.20}$$

Terminologies of *left* and *right* have a sense if we assume the movement to the direction of $\mathbf{e}_1$. Throughout this chapter, whenever required, upper and lower signs refer to the left and right quantities, respectively. The origin is in the middle in

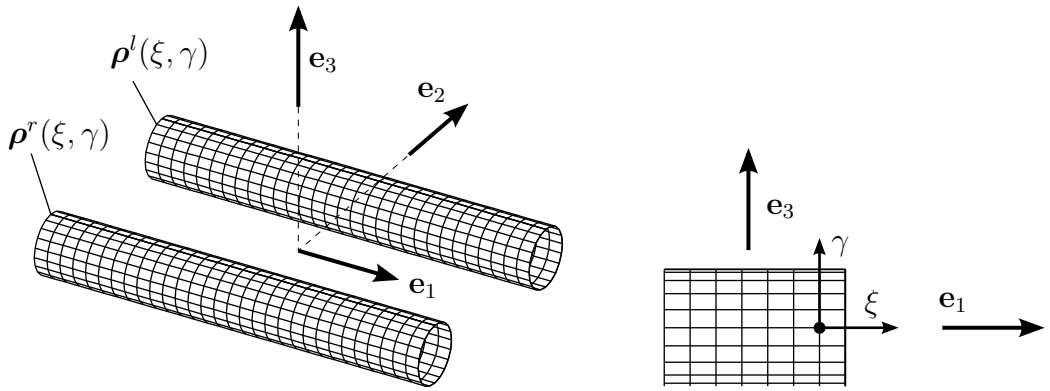

Figure 2.8: Surface model of the rails

the common plane of the axes of the cylinders. Here ξ is the surface parameter increasing along the direction of the rails. The γ surface parameter shows the angle around the cylinder, $\gamma = 0$ corresponds to the top of the rails. Their ranges are:

$$\begin{aligned} \xi &\in (-\infty, \infty) \\ \gamma &\in [-\pi, \pi) \end{aligned} \tag{2.2.21}$$

The surface of the wheelset is modelled with a bicone, the base radius R and, the half of the conical angle is α, and $h := \tan\alpha$. The surface is described by $\boldsymbol{\kappa}$, which is given by basis $\mathbf{h}_i$ fixed to the wheelset. Let

$$\mathbf{h}_i^* \boldsymbol{\kappa}(\chi, \delta) := \mathbf{h}_i^* \mathbf{x} + \begin{bmatrix} c(\chi)\sin(\delta) \\ \chi \\ c(\chi)\cos(\delta) \end{bmatrix}, \tag{2.2.22}$$

where the directrix of the bicone is

$$c(\chi) := \begin{Bmatrix} -R + h\chi & \text{if} & \chi \geq 0 \\ -R - h\chi & \text{if} & \chi \leq 0 \end{Bmatrix} \tag{2.2.23}$$

Here χ is the surface parameter which measures the distance on the symmetry axis, and the angle δ generates the axisymmetric geometry from the directrix $c(\chi)$. The value $\chi = 0$ shows the symmetry plane of the bicone, and the $\delta = 0$ is the lowest directrix of the bicone in natural position. The range of the parameters are:

$$\begin{aligned} \chi &\in (-R/h, R/h) \\ \delta &\in (-\pi, \pi) \end{aligned} \tag{2.2.24}$$

It can be seen from (2.2.22), that the vector $\mathbf{x}$ of the pivot point is in the geometric centre of the bicone.

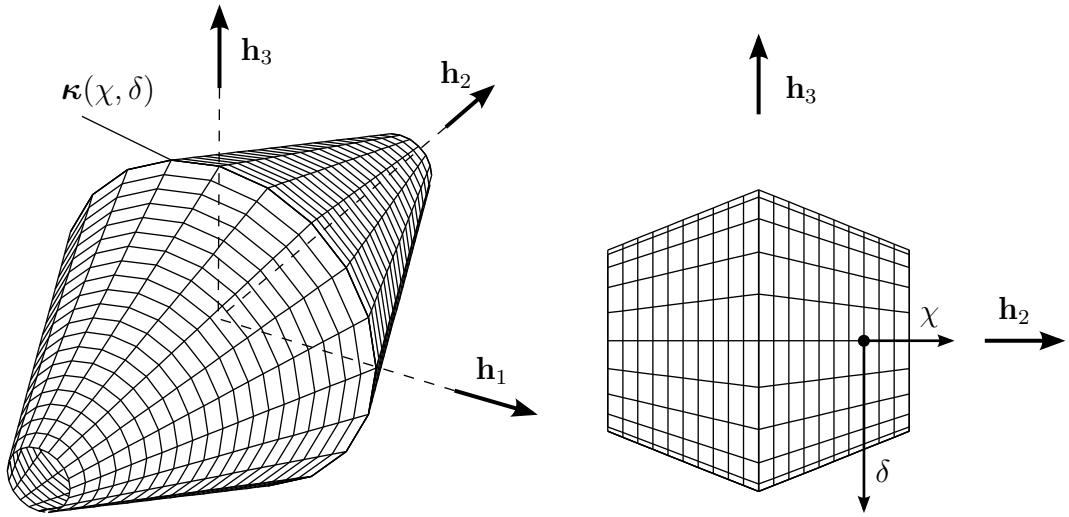

Figure 2.9: Surface model of the wheelset

2.2.4 Constraints

It is not easy to implement the constraints directly for the q^u variable, but the parametric definition of the surfaces provides a straightforward way for it. The main idea is to follow the surface coordinates during the motion with additional variables. With this method first the configuration space is extended with the surface coordinates of the contact points, then with appropriate number of constraint equations, these new variables and some of the old ones are eliminated simultaneously.

Let us call the contact points *left* and *right* contact points according to the rails. The surface coordinates of the left contact point are denoted by ξ^l and γ^l on the left rail, and χ^l, δ^l on the wheelset. The coordinates of the right contact point is denoted similarly just with an upper index r.

These quantities are considered to be functions of time and they correspond to the state of the system. Therefore we can add them to the variables and an extended state variable of the unconstrained system is obtained:

$$q^e = (x, y, z, \varphi, \psi, \vartheta, \xi^l, \gamma^l, \chi^l, \delta^l, \xi^r, \gamma^r, \chi^r, \delta^r) \in \mathbb{R}^{14} \tag{2.2.25}$$

Of course this 14-dimensional space is redundant, although (2.2.19) was so too without applying the constraints.

After introducing these new variables the constraints can be implemented easily. First let us consider that the contact points must have coincidence on the two

contacting bodies. Therefore

$$\begin{aligned} \boldsymbol{\kappa}(\chi^l, \delta^l) &\doteq \boldsymbol{\rho}^l(\xi^l, \gamma^l) \\ \boldsymbol{\kappa}(\chi^r, \delta^r) &\doteq \boldsymbol{\rho}^r(\xi^r, \gamma^r) \end{aligned} \tag{2.2.26}$$

have to be satisfied.

The surfaces are not just touching each other but they are in tangential connection at the contact points. This can be mathematically expressed by the equality of the tangent spaces of the surfaces at the contact points. Thus

$$\begin{aligned} \mathrm{T}_{(\chi^l,\delta^l)}\boldsymbol{\kappa} &\doteq \mathrm{T}_{(\xi^l,\gamma^l)}\boldsymbol{\rho}^l \\ \mathrm{T}_{(\chi^r,\delta^r)}\boldsymbol{\kappa} &\doteq \mathrm{T}_{(\xi^r,\gamma^r)}\boldsymbol{\rho}^r \end{aligned} \tag{2.2.27}$$

have to be fulfilled where $\mathrm{T}_x f$ denotes the tangent space of the function f at a point x.

The coincidence constraints in (2.2.26) are vector equations, therefore each means three scalar equations. However the tangent constraints in (2.2.27) mean two scalar equations for each. We can see later, that all of these scalar equations are independent, they altogether reduce the number of the variables by 3+3+2+2 = 10.

We assume ideal rolling, and the rails are fixed, hence the velocity of the wheelset must be zero at the contact points:

$$\begin{aligned} \mathbf{v} \circ \boldsymbol{\kappa}(\chi^l, \delta^l) &\doteq \mathbf{0} \\ \mathbf{v} \circ \boldsymbol{\kappa}(\chi^r, \delta^r) &\doteq \mathbf{0} \end{aligned}, \tag{2.2.28}$$

where $\circ$ denotes the composition of functions. The two rolling constraints would mean theoretically 6 scalar equations, but their independence from each other and from the geometric constraints in (2.2.26)-(2.2.27) has to be explored. We will see that the rolling constraints add only 3 more independent equations to the geometric equations.

Up to this point the constraints has described the contact between the wheelset and the rails. The last constraint is completely independent from them and it has been introduced as a load. The speed of the rail vehicle is considered to be constant v, and the geometric centre of the gravity of the wheelset can be assumed to move with this constant velocity along the rails. This can be included into the equation:

$$\mathbf{e}_1^* \mathbf{v} \circ \mathbf{x} = v \tag{2.2.29}$$

Constraints are usually classified as holonomic and non-holonomic constraints, which definitions contain properties of integrability. For our purposes it is more

straightforward to distinguish *geometric* constraints, which provide restrictions between the variables in (2.2.25) and *kinematic* constraints which contains restrictions also for the derivatives of the variables. From this point of view (2.2.26) and (2.2.27) are geometric, (2.2.28) and (2.2.29) are kinematic constraints.

2.3 Derivation of the equations of motion

In this section our aim is to calculate the differential equations of the system. First the geometric constraints (tangent and coincidence) are applied to restrict the variables, then we consider the kinematic constraints (rolling and pulling) restricting the velocities. It turns out that we do not need Newtonian equations to derive the differential equations, because the constraints determine the motion of the system.

Although the coincidence constraints are more fundamental physically, it is better to begin with the tangent constraints, because they can be solved separately and some of the variables can be eliminated immediately.

2.3.1 Tangent constraint

There are several ways of applying the requirement of common tangent space of two surfaces. The parallelism of the normal vectors could be examined or the perpendicularity of a normal vector with the tangent vectors of the other surface could be described.

In the following let us use the property, that if the tangent space is common at the contact point, then all the possible tangent vectors of the surfaces must be in the same plane. It is easy to calculate the normal vectors generated by partial differentiation respect to the surface parameters. If the coordinate net of a surface has no singularity at the contact point, then the partial derivatives span the tangent space. Therefore it is enough to check for each contact point, that any three from the four partial derivative vectors are in the same plane.

The calculations are made simultaneously with the left and right contact points. The derivatives are calculated in the own bases of the bodies then they are transformed to an appropriate common system to apply the constraints.

The partial derivatives of the rails at the contact points:

$$\mathbf{e}_i^*(\partial_1\boldsymbol{\rho}^{lr})(\xi,\gamma) = \begin{bmatrix}1\\0\\0\end{bmatrix} \tag{2.3.1}$$

$$\mathbf{e}_i^*(\partial_2\boldsymbol{\rho}^{lr})(\xi,\gamma) = \begin{bmatrix}0\\r\cos\gamma\\-r\sin\gamma\end{bmatrix} \tag{2.3.2}$$

The partial derivatives of the bicone in its own basis:

$$\mathbf{h}_i^*(\partial_1\boldsymbol{\kappa})(\chi,\delta) = \begin{bmatrix}c'(\chi)\sin\delta\\1\\c'(\chi)\cos\delta\end{bmatrix} \tag{2.3.3}$$

$$\mathbf{h}_i^*(\partial_2\boldsymbol{\kappa})(\chi,\delta) = \begin{bmatrix}c(\chi)\cos\delta\\0\\-c(\chi)\sin\delta\end{bmatrix} \tag{2.3.4}$$

The four vectors are all transformed to the basis denoted by $\mathbf{g}_i$ in order to simplify the calculations:

$$\mathbf{g}_i^*(\partial_1\boldsymbol{\rho}^{lr})(\xi,\gamma) = Q_{ij}^{-1}(\psi)P_{jk}^{-1}(\vartheta)\mathbf{e}_k^*(\partial_1\boldsymbol{\rho}^{lr})(\xi,\gamma) = \begin{bmatrix}\cos\psi\\-\sin\psi\\0\end{bmatrix} \tag{2.3.5}$$

$$\mathbf{g}_i^*(\partial_2\boldsymbol{\rho}^{lr})(\xi,\gamma) = Q_{ij}^{-1}(\psi)P_{jk}^{-1}(\vartheta)\mathbf{e}_k^*(\partial_2\boldsymbol{\rho}^{lr})(\xi,\gamma) = \begin{bmatrix}r\sin\psi\cos(\vartheta+\gamma)\\r\cos\psi\cos(\vartheta+\gamma)\\-r\sin(\vartheta+\gamma)\end{bmatrix} \tag{2.3.6}$$

$$\mathbf{g}_i^*(\partial_1\boldsymbol{\kappa})(\chi,\delta) = R_{ij}(\varphi)\mathbf{h}_j^*(\partial_1\boldsymbol{\kappa})(\chi,\delta) = \begin{bmatrix}c'(\chi)\sin(\varphi+\delta)\\1\\c'(\chi)\cos(\varphi+\delta)\end{bmatrix} \tag{2.3.7}$$

$$\mathbf{g}_i^*(\partial_2\boldsymbol{\kappa})(\chi,\delta) = R_{ij}(\varphi)\mathbf{h}_j^*(\partial_2\boldsymbol{\kappa})(\chi,\delta) = \begin{bmatrix}c(\chi)\cos(\varphi+\delta)\\0\\-c(\chi)\sin(\varphi+\delta)\end{bmatrix} \tag{2.3.8}$$

The linear dependence of three vectors can be examined by evaluating the triple scalar product of them. If three vectors are linearly dependent, then the

triple product must be zero. The triple product can be calculated easily from the matrix composed from the vectors. Hence (2.2.27) becomes

$$\det\left[\mathbf{g}_i^*(\partial_1\boldsymbol{\kappa})(\chi^{lr},\delta^{lr}) \quad \mathbf{g}_i^*(\partial_2\boldsymbol{\kappa})(\chi^{lr},\delta^{lr}) \quad \mathbf{g}_i^*(\partial_1\boldsymbol{\rho}^{lr})(\xi^{lr},\gamma^{lr})\right]=0 \tag{2.3.9}$$

$$\det\left[\mathbf{g}_i^*(\partial_1\boldsymbol{\kappa})(\chi^{lr},\delta^{lr}) \quad \mathbf{g}_i^*(\partial_2\boldsymbol{\kappa})(\chi^{lr},\delta^{lr}) \quad \mathbf{g}_i^*(\partial_2\boldsymbol{\rho}^{lr})(\xi^{lr},\gamma^{lr})\right]=0 \tag{2.3.10}$$

These equations contain the linear dependence of the four vectors in both points.

Let us first calculate (2.3.9). After substitution of the derivatives the equation becomes

$$\begin{vmatrix} c'(\chi^{lr})\sin(\varphi+\delta^{lr}) & c(\chi^{lr})\cos(\varphi+\delta^{lr}) & \cos\psi \\ 1 & 0 & -\sin\psi \\ c'(\chi^{lr})\cos(\varphi+\delta^{lr}) & -c(\chi^{lr})\sin(\varphi+\delta^{lr}) & 0 \end{vmatrix}=0. \tag{2.3.11}$$

Calculating the determinant:

$$-c(\chi^{lr})\left(\sin(\varphi+\delta^{lr})\cos\psi+c'(\chi^{lr})\sin\psi\right)=0 \tag{2.3.12}$$

Let us suppose that the contact points are on different cones of the bicone, that is

$$\chi^l>0 \qquad\qquad \chi^r<0 \tag{2.3.13}$$

This causes $c'(\chi^{lr})=\pm h$. By substituting (2.2.24) into (2.2.23) we can be ensured that $c(\chi^{lr})>0$ Therefore (2.3.12) gives:

$$\boxed{\sin(\varphi+\delta^{lr})=\mp h\tan\psi} \tag{2.3.14}$$

This is useful to understand the meaning of the $\varphi+\delta^{lr}$ angle. As the body is axysymmetric, a change only in the rolling angle φ has the same effect on the system as a same change only in the δ variable. Therefore none of them, only their sum can have direct geometric meaning. They together determine the directrices on both half-cones, which contain the contact points, and the angle of these directrices is measured from the $\psi=0$ natural position.

Equation (2.3.14) contains a restriction to the ψ angle, as the absolute value of the sine function must be smaller or equal than one. From this we get:

$$|\tan\psi|<\frac{1}{h} \tag{2.3.15}$$

In the physical relevant case $|\varphi+\delta^{lr}|<\pi/2$, therefore:

$$\boxed{\cos(\varphi+\delta^{lr})=\sqrt{1-h^2\tan^2\psi}} \tag{2.3.16}$$

Let us now calculate the other part of the tangent constraint in (2.3.10):

$$\begin{vmatrix} c'(\chi^{lr})\sin(\varphi+\delta^{lr}) & c(\chi^{lr})\cos(\varphi+\delta^{lr}) & r\sin\psi\cos(\vartheta+\gamma^{lr}) \\ 1 & 0 & r\cos\psi\cos(\vartheta+\gamma^{lr}) \\ c'(\chi^{lr})\cos(\varphi+\delta^{lr}) & -c(\chi^{lr})\sin(\varphi+\delta^{lr}) & -r\sin(\vartheta+\gamma^{lr}) \end{vmatrix} = 0 \qquad (2.3.17)$$

During calculation of the determinant (2.3.14) and (2.3.16) can be already used:

$$rc(\chi^{lr})\left(\frac{\pm h}{\cos\psi}\cos(\vartheta+\gamma^{lr})+\sqrt{1-h^2\tan^2\psi}\,\sin(\vartheta+\gamma^{lr})\right)=0 \qquad (2.3.18)$$

In the physically realistic case we can assume that $|\vartheta+\gamma^{lr}|<\pi/2$. With this we find:

$$\boxed{\sin(\vartheta+\gamma^{lr})=\frac{\mp h}{\cos\psi\sqrt{1+h^2}}} \qquad (2.3.19)$$

$$\boxed{\cos(\vartheta+\gamma^{lr})=\frac{\sqrt{1-h^2\tan^2\psi}}{\sqrt{1+h^2}}} \qquad (2.3.20)$$

One can check that if condition (2.3.15) is satisfied, then the right-hand side of these equations must remain below one in absolute value.

The tangent constraints have been applied, and finally (2.3.14)-(2.3.16) and (2.3.19)-(2.3.20) are obtained. From this four variables, γ^l, γ^r, δ^l and δ^r could be calculated, but it is unnecessary as the following derivations can be done with using directly the sum of these angles.

2.3.2 Coincidence constraint

For the calculation of the coincidence constraints (2.2.26), the functions of the surfaces should be transformed to a common coordinate system. Bases $(\mathbf{g}_i)$ or $(\mathbf{f}_i)$ can be used easily, but the second one leads to simpler formulae.

Let us transform the function of the rail in (2.2.20) to the coordinate system defined by basis $(\mathbf{f}_i)$:

$$\mathbf{f}_i^*\boldsymbol{\rho}^{lr}(\xi,\gamma)=P_{ij}^{-1}(\vartheta)\mathbf{e}_j^*\boldsymbol{\rho}^{lr}(\xi,\gamma)=\begin{bmatrix}\xi\\ r\sin(\vartheta+\gamma)\pm d\cos\vartheta\\ r\cos(\vartheta+\gamma)\mp d\sin\vartheta\end{bmatrix} \qquad (2.3.21)$$

Let us consider the contact points and let us use the results from (2.3.19)-(2.3.20) to get:

$$\mathbf{f}_i^*\boldsymbol{\rho}^{lr}(\xi^{lr},\gamma^{lr})=\begin{bmatrix}\xi^{lr}\\ \pm\left(d\cos\psi\cos\vartheta-\frac{rh}{\sqrt{1+h^2}}\right)\frac{1}{\cos\psi}\\ \mp d\sin\vartheta+\frac{r\sqrt{1-h^2\tan^2\psi}}{\sqrt{1+h^2}}\end{bmatrix} \qquad (2.3.22)$$

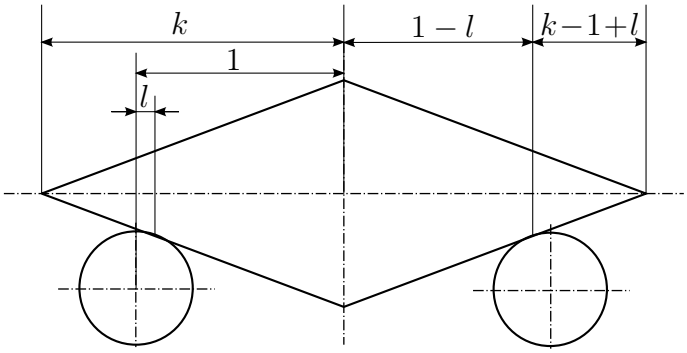

Figure 2.10: Dimensionless parameters. In the figure all lengths are resized by d to get the dimensionless quantities. Terms $k-1+l$ and $1-l$ appear often in the calculations and also in the final form of the differential equation. Comparing with Figure 1.5, $\hat{d}/d = 1-l$ and $\hat{R}/d = h(k-1+l)$.

The equation of the bicone is also transformed to the $\mathbf{f}_i$ basis:

$$\mathbf{f}_i^* \boldsymbol{\kappa}(\chi,\delta) = Q_{ij}(\psi)R_{jk}(\varphi)\mathbf{h}_k^* \boldsymbol{\kappa}(\chi,\delta) = \\ = \begin{bmatrix} c(\chi)\sin(\varphi+\delta)\cos\psi - \chi\sin\psi \\ c(\chi)\sin(\varphi+\delta)\sin\psi + \chi\cos\psi \\ c(\chi)\cos(\varphi+\delta) \end{bmatrix} + \mathbf{f}_i^*\mathbf{x} \quad (2.3.23)$$

Substituting the contact points again, and using (2.3.14)-(2.3.16) we obtain:

$$\mathbf{f}_i^* \boldsymbol{\kappa}(\chi^{lr},\delta^{lr}) = \begin{bmatrix} -\sin\psi\big((1+h^2)\chi^{lr} \pm Rh\big) \\ \cos\psi\left((1-h^2\tan^2\psi)\chi^{lr} \pm Rh\tan^2\psi\right) \\ -R\sqrt{1-h^2\tan^2\psi} \pm \chi^{lr}h\sqrt{1-h^2\tan^2\psi} \end{bmatrix} + \mathbf{f}_i^*\mathbf{x} \quad (2.3.24)$$

The constraints in (2.2.26) are not used directly, but rather their sum and difference is examined to utilize the symmetries of the left and right sides:

$$\boldsymbol{\rho}^l(\xi^l,\gamma^l) - \boldsymbol{\rho}^r(\xi^r,\gamma^r) = \boldsymbol{\kappa}(\chi^l,\delta^l) - \boldsymbol{\kappa}(\chi^r,\delta^r) \quad (2.3.25)$$

$$\boldsymbol{\rho}^l(\xi^l,\gamma^l) + \boldsymbol{\rho}^r(\xi^r,\gamma^r) = \boldsymbol{\kappa}(\chi^l,\delta^l) + \boldsymbol{\kappa}(\chi^r,\delta^r) \quad (2.3.26)$$

Before performing the calculations let us introduce the following new parameters:

$$k := \frac{R}{dh} \qquad\qquad l := \frac{rh}{d\sqrt{1+h^2}} \quad (2.3.27)$$

Parameters k and l are introduced to simplify the expressions, but they have geometrical meaning according to Figure 2.10.

Let us produce the two sides of (2.3.25) in our current coordinate system $\mathbf{f}_i$. To simplify the calculations, the equations are divided by $2d$:

$$\frac{\mathbf{f}_i^*\boldsymbol{\rho}^l(\xi^l,\gamma^l)-\mathbf{f}_i^*\boldsymbol{\rho}^r(\xi^r,\gamma^r)}{2d}=\begin{bmatrix}\frac{\xi^l-\xi^r}{2d}\\(\cos\psi\cos\vartheta-l)\,\frac{1}{\cos\psi}\\-\sin\vartheta\end{bmatrix} \tag{2.3.28}$$

$$\frac{\mathbf{f}_i^*\boldsymbol{\kappa}(\chi^l,\delta^l)-\mathbf{f}_i^*\boldsymbol{\kappa}(\chi^r,\delta^r)}{2d}=\begin{bmatrix}-\sin\psi\left(\frac{\chi^l-\chi^r}{2d}(1+h^2)+kh^2\right)\\\cos\psi\left(\frac{\chi^l-\chi^r}{2d}(1-h^2\tan^2\psi)+kh^2\tan^2\psi\right)\\\frac{\chi^l+\chi^r}{2d}h\sqrt{1-h^2\tan^2\psi}\end{bmatrix} \tag{2.3.29}$$

After equalizing them, the following results can be obtained:

$$\boxed{\frac{\chi^l-\chi^r}{2d}=\frac{(\cos\vartheta\cos\psi-l)-kh^2\sin^2\psi}{\cos^2\psi(1-h^2\tan^2\psi)}} \tag{2.3.30}$$

$$\boxed{\frac{\chi^l+\chi^r}{2d}=\frac{-\sin\vartheta}{h\sqrt{1-h^2\tan^2\psi}}} \tag{2.3.31}$$

$$\boxed{\frac{\xi^l-\xi^r}{2d}=-\sin\psi\frac{(\cos\vartheta\cos\psi-l)\,(1+h^2)-kh^2}{\cos^2\psi(1-h^2\tan^2\psi)}} \tag{2.3.32}$$

Then let us work out the left-hand side of the another equation in (2.3.26):

$$\frac{\mathbf{f}_i^*\boldsymbol{\rho}^l(\xi^l,\gamma^l)+\mathbf{f}_i^*\boldsymbol{\rho}^r(\xi^r,\gamma^r)}{2d}=\begin{bmatrix}\frac{\xi^l+\xi^r}{2d}\\0\\\frac{l}{h}\sqrt{1-h^2\tan^2\psi}\end{bmatrix} \tag{2.3.33}$$

To the right-hand side also (2.3.31) and (2.3.30) are substituted:

$$\frac{\mathbf{f}_i^*\boldsymbol{\kappa}(\chi^l,\delta^l)+\mathbf{f}_i^*\boldsymbol{\kappa}(\chi^r,\delta^r)}{2d}=\begin{bmatrix}-\frac{\chi^l+\chi^r}{2d}(1+h^2)\sin\psi\\\frac{\chi^l+\chi^r}{2d}(1-h^2\tan^2\psi)\cos\psi\\-kh\sqrt{1-h^2\tan^2\psi}+\frac{\chi^l-\chi^r}{2d}h\sqrt{1-h^2\tan^2\psi}\end{bmatrix}+$$

$$+\frac{\mathbf{f}_i^*\mathbf{x}}{d}=\begin{bmatrix}\frac{\sin\vartheta\sin\psi(1+h^2)}{h\sqrt{1-h^2\tan^2\psi}}\\\frac{-\sin\vartheta\cos\psi(1-h^2\tan^2\psi)}{h\sqrt{1-h^2\tan^2\psi}}\\\frac{(\cos\vartheta\cos\psi-l)h^2-kh^2\cos^2\psi}{\cos^2\psi h\sqrt{1-h^2\tan^2\psi}}\end{bmatrix}+\frac{\mathbf{f}_i^*\mathbf{x}}{d} \tag{2.3.34}$$

Using (2.3.26) $\mathbf{f}_i^*\mathbf{x}$ can be expressed:

$$\frac{\mathbf{f}_i^*\mathbf{x}}{d}=\begin{bmatrix}\frac{\xi^l+\xi^r}{2d}-\frac{\sin\vartheta\sin\psi(1+h^2)}{h\sqrt{1-h^2\tan^2\psi}}\\\frac{\sin\vartheta\cos\psi(\cos^2\psi-h^2\sin^2\psi)}{\cos^2\psi h\sqrt{1-h^2\tan^2\psi}}\\\frac{-h^2\cos\vartheta\cos\psi+l(1+h^2)\cos^2\psi+kh^2\cos^2\psi}{\cos^2\psi h\sqrt{1-h^2\tan^2\psi}}\end{bmatrix} \tag{2.3.35}$$

Transforming it to the outer coordinate system:

$$\frac{\mathbf{e}_i^*\mathbf{x}}{d} = P_{ij}(\vartheta)\frac{\mathbf{f}_j^*\mathbf{x}}{d} = \begin{bmatrix} \frac{\xi^l+\xi^r}{2d} - \frac{\sin\vartheta\sin\psi(1+h^2)}{h\sqrt{1-h^2\tan^2\psi}} \\ \sin\vartheta\frac{(\cos\vartheta\cos\psi-l)(1+h^2)-kh^2}{h\sqrt{1-h^2\tan^2\psi}} \\ \frac{\cos\psi\sqrt{1-h^2\tan^2\psi}}{h} - \cos\vartheta\frac{(\cos\vartheta\cos\psi-l)(1+h^2)-kh^2}{h\sqrt{1-h^2\tan^2\psi}} \end{bmatrix} \tag{2.3.36}$$

Which comparing to (2.2.12) gives:

$$\boxed{\frac{\xi^l+\xi^r}{2d} = \frac{x}{d} + \frac{\sin\vartheta\sin\psi(1+h^2)}{h\sqrt{1-h^2\tan^2\psi}}} \tag{2.3.37}$$

$$\boxed{\frac{y}{d} = \sin\vartheta\frac{(\cos\vartheta\cos\psi-l)(1+h^2)-kh^2}{h\sqrt{1-h^2\tan^2\psi}}} \tag{2.3.38}$$

$$\boxed{\frac{z}{d} = \frac{\cos\psi\sqrt{1-h^2\tan^2\psi}}{h} - \cos\vartheta\frac{(\cos\vartheta\cos\psi-l)(1+h^2)-kh^2}{h\sqrt{1-h^2\tan^2\psi}}} \tag{2.3.39}$$

With the help of equations (2.3.30)-(2.3.32) and (2.3.37)-(2.3.39) now ξ^l, ξ^r, χ^l, χ^r, y and z variables can be eliminated. Other variables could also be chosen for expression but this choice seems to be the simplest. Considering also the tangent constraint, all of our variables in (2.2.25) can be expressed using the three Euler angles and x. Therefore the new variables after using the constraints:

$$q^c := (x, \varphi, \psi, \vartheta) \in \mathbb{R}^4 \tag{2.3.40}$$

Thus after applying the geometric constraints a four-dimensional configuration space is obtained, in other words four general coordinates can be used for describing our system. It is important that the coordinates of the contact points are absent from q^c as there was planned at the beginning of the section. The physical meaning of the remaining variables are straightforward: x and φ describe the natural motion of the wheel, ϑ and ψ characterize the hunting motion.

2.3.3 Rolling and pulling constraints

Similar to the coincidence constraint, not equations in (2.2.28) are examined directly, but their sum and difference. After making this transformation and substituting the velocity function from (2.2.11) we get:

$$\boldsymbol{\Omega}\left(\boldsymbol{\kappa}(\chi^l,\delta^l) - \boldsymbol{\kappa}(\chi^r,\delta^r)\right) = \mathbf{0} \tag{2.3.41}$$

and

$$\mathbf{\Omega}\left(\boldsymbol{\kappa}(\chi^l,\delta^l)+\boldsymbol{\kappa}(\chi^r,\delta^r)-2\mathbf{x}\right)+2\dot{\mathbf{x}}=\mathbf{0} \tag{2.3.42}$$

For applying the constraints the angular velocity tensor is to be determined. It can be done according to the definition in (2.2.11):

$$\begin{aligned}\mathbf{e}_i^*\mathbf{\Omega}\mathbf{e}_j&=\mathbf{e}_i^*\dot{\mathbf{R}}\mathbf{R}^*\mathbf{e}_j=\\&=\begin{bmatrix}0&-\dot\varphi\cos\psi\sin\vartheta-\dot\psi\cos\vartheta&\dot\varphi\cos\psi\cos\vartheta-\dot\psi\sin\vartheta\\\dot\varphi\cos\psi\sin\vartheta+\dot\psi\cos\vartheta&0&-\dot\vartheta+\dot\varphi\sin\psi\\-\dot\varphi\cos\psi\cos\vartheta+\dot\psi\sin\vartheta&\dot\vartheta-\dot\varphi\sin\psi&0\end{bmatrix}\end{aligned} \tag{2.3.43}$$

The calculation is more simple if we transform it to basis $(\mathbf{f}_i)$:

$$\mathbf{f}_i^*\mathbf{\Omega}\mathbf{f}_j=P_{ik}^{-1}(\vartheta)\mathbf{e}_k^*\mathbf{\Omega}\mathbf{e}_lP_{lj}(\vartheta)=\begin{bmatrix}0&-\dot\psi&\dot\varphi\cos\psi\\\dot\psi&0&-\dot\vartheta+\dot\varphi\sin\psi\\-\dot\varphi\cos\psi&\dot\vartheta-\dot\varphi\sin\psi&0\end{bmatrix} \tag{2.3.44}$$

Equation (2.3.41) can be rewritten using (2.3.25):

$$\frac{\mathbf{\Omega}\boldsymbol{\rho}^l(\xi^l,\gamma^l)-\mathbf{\Omega}\boldsymbol{\rho}^r(\xi^r,\gamma^r)}{2d}=\mathbf{0} \tag{2.3.45}$$

The final form of the difference of the contact points using all geometric constraints:

$$\frac{\mathbf{e}_i^*\boldsymbol{\rho}^l(\xi^l,\gamma^l)-\mathbf{e}_i^*\boldsymbol{\rho}^r(\xi^r,\gamma^r)}{2d}=\begin{bmatrix}-\sin\psi\frac{(\cos\vartheta\cos\psi-l)(1+h^2)-kh^2}{\cos^2\psi(1-h^2\tan^2\psi)}\\(\cos\psi\cos\vartheta-l)\frac{1}{\cos\psi}\\-\sin\vartheta\end{bmatrix}=:\begin{bmatrix}v_1\\v_2\\v_3\end{bmatrix} \tag{2.3.46}$$

The v_1-v_3 notations are introduced in order to shorten the calculation. Substituting this into (2.3.45) we get:

$$\begin{bmatrix}0&-\dot\psi&\dot\varphi\cos\psi\\\dot\psi&0&-\dot\vartheta+\dot\varphi\sin\psi\\-\dot\varphi\cos\psi&\dot\vartheta-\dot\varphi\sin\psi&0\end{bmatrix}\cdot\begin{bmatrix}v_1\\v_2\\v_3\end{bmatrix}=\begin{bmatrix}0\\0\\0\end{bmatrix} \tag{2.3.47}$$

Let us create a system of linear equations from this equation:

$$\begin{bmatrix}0&-v_2&v_3\cos\psi\\-v_3&v_1&v_3\sin\psi\\v_2&0&-v_2\sin\psi-v_1\cos\psi\end{bmatrix}\cdot\begin{bmatrix}\dot\vartheta\\\dot\psi\\\dot\varphi\end{bmatrix}=\begin{bmatrix}0\\0\\0\end{bmatrix} \tag{2.3.48}$$

It can be checked that the rank of the coefficient matrix is 2, therefore only two of the three constraint equations are independent. Any two of the three equations can be chosen. For the simplicity the first and third are picked:

$$-\dot\psi v_2+\dot\varphi v_3\cos\psi=0 \tag{2.3.49}$$

$$\dot{\vartheta}v_2 - \dot{\varphi}(v_1 \cos\psi + v_2 \sin\psi) = 0 \tag{2.3.50}$$

Substituting these back into the definitions of the v_1-v_3 components and after some manipulation:

$$\boxed{\dot{\psi}\frac{\cos\vartheta\cos\psi - l}{\cos^2\psi} + \dot{\varphi}\sin\vartheta = 0} \tag{2.3.51}$$

$$\boxed{\dot{\varphi}h^2\left(k - \frac{\cos\vartheta\cos\psi - l}{\cos^2\psi}\right)\sin\psi - \dot{\vartheta}\frac{\cos\vartheta\cos\psi - l}{\cos^2\psi}(1 - h^2\tan^2\psi) = 0} \tag{2.3.52}$$

For calculating (2.3.42) the appropriate expression for the distance is needed from (2.3.34):

$$\frac{\mathbf{f}_i^*\boldsymbol{\kappa}(\chi^l,\delta^l) + \mathbf{f}_i^*\boldsymbol{\kappa}(\chi^r,\delta^r)}{2d} - \frac{\mathbf{f}_i^*\mathbf{x}}{d} = \begin{bmatrix} \frac{\sin\vartheta\sin\psi(1+h^2)}{h\sqrt{1-h^2\tan^2\psi}} \\ \frac{-\sin\vartheta\cos\psi(1-h^2\tan^2\psi)}{h\sqrt{1-h^2\tan^2\psi}} \\ \frac{(\cos\vartheta\cos\psi - l)h^2 - kh^2\cos^2\psi}{\cos^2\psi h\sqrt{1-h^2\tan^2\psi}} \end{bmatrix} =: \begin{bmatrix} v_4 \\ v_5 \\ v_6 \end{bmatrix} \tag{2.3.53}$$

Also the velocity of the centre of the wheelset is to be calculated:

$$\mathbf{f}_i^*\mathbf{x} = P_{ij}^{-1}(\vartheta)\mathbf{e}_j^*\mathbf{x} = \begin{bmatrix} \dot{x} \\ \dot{y}\cos\vartheta + \dot{z}\sin\vartheta \\ \dot{z}\cos\vartheta - \dot{y}\sin\vartheta \end{bmatrix} \tag{2.3.54}$$

Substituting back into (2.3.42):

$$\begin{bmatrix} 0 & -\dot{\psi} & \dot{\varphi}\cos\psi \\ \dot{\psi} & 0 & -\dot{\vartheta} + \dot{\varphi}\sin\psi \\ -\dot{\varphi}\cos\psi & \dot{\vartheta} - \dot{\varphi}\sin\psi & 0 \end{bmatrix}\begin{bmatrix} v_4 \\ v_5 \\ v_6 \end{bmatrix} + \frac{1}{d}\begin{bmatrix} \dot{x} \\ \dot{y}\cos\vartheta + \dot{z}\sin\vartheta \\ \dot{z}\cos\vartheta - \dot{y}\sin\vartheta \end{bmatrix} = 0 \tag{2.3.55}$$

It can be seen immediately that the second and third scalar equations are not independent from the coincidence constraint, they can be obtained by differentiation of (2.3.38) and (2.3.39) with respect to time. This is not surprising because the coincidence constraints have to ensure the zero relative velocity at the contact point in the normal direction of the surfaces. Therefore only one scalar equation can be obtained from the first row of the vector equation:

$$\dot{\varphi}\cos\psi v_6 - \dot{\psi}v_5 + \frac{\dot{x}}{d} = 0 \tag{2.3.56}$$

After substitution:

$$\boxed{-\dot{\varphi}h^2\left(k - \frac{\cos\vartheta\cos\psi - l}{\cos^2\psi}\right) + \dot{\psi}\sin\vartheta(1 - h^2\tan^2\psi) + h\frac{\dot{x}}{d} = 0} \tag{2.3.57}$$

Finally we found, that from the six of the rolling constraint equations only three are independent from each other and from the geometric constraints, these lead to equations (2.3.51), (2.3.52) and (2.3.57).

The calculation of the constant pulling speed of the wheelset is clearly the simplest one compared to the previous constraints. Let us calculate (2.2.29) to obtain:

$$\boxed{\dot{x} = v} \tag{2.3.58}$$

2.3.4 Equations of motion of the system

We have applied all kinematic constraints, and got equations (2.3.51), (2.3.52), (2.3.57) and (2.3.58). These kinematic equations mean four independent linear equations for $\dot{\vartheta}$, $\dot{\psi}$,$\dot{\varphi}$ and $\dot{x}$. These equations can be solved, and these derivatives can be expressed explicitly as functions of the general coordinates.

This fact means that all of the time derivatives become known at a given point of the configuration space. Hence Newton's Second Law is not needed to derive the differential equations, they can be derived from the dynamical constraint equations.

Thus for (2.3.51), (2.3.52), (2.3.57) and (2.3.58) we find

$$\boxed{\begin{aligned}
\dot{x} &= v && (2.3.59)\\
\dot{\varphi} &= \frac{\cos\vartheta\cos\psi - l}{\cos^2\psi}\cdot S(\psi,\vartheta) && (2.3.60)\\
\dot{\psi} &= -\sin\vartheta\cdot S(\psi,\vartheta) && (2.3.61)\\
\dot{\vartheta} &= \frac{h^2\sin\psi}{1-h^2\tan^2\psi}\left(k - \frac{\cos\vartheta\cos\psi - l}{\cos^2\psi}\right)\cdot S(\psi,\vartheta) && (2.3.62)
\end{aligned}}$$

where the

$$S(\psi,\vartheta) := \frac{V}{\frac{\cos\vartheta\cos\psi - l}{\cos^2\psi}\left(k - \frac{\cos\vartheta\cos\psi - l}{\cos^2\psi}\right)h^2 + \sin^2\vartheta(1-h^2\tan^2\psi)} \tag{2.3.63}$$

function is introduced for shorthand notation, and

$$V := \frac{vh}{d} \tag{2.3.64}$$

is the dimensionless velocity.

Therefore we have obtained the equations of the motion of the system. It is very comfortable that due to the lack of the second-order Newtonian equations it is already a system of first-order differential equations, thus the general coordinates

become phase variables and the configuration space is equivalent with the phase space.

If we consider the system in the point o f view of the Appell-equations (see Gantmacher [2], p. 61.), this result is not surprising. If an n-dimensional configuration space is exposed to m kinematic constraints, then a $2n - m$-dimensional system of equations can be obtained. This system consists of $n - m$ scalar Appell equations, $n - m$ equations from the definitions of the pseudo-velocities and m equations from the kinematic constraints. As we have $n = m = 4$, there are only equations from the constrains.

In the next chapter these equations are going to be investigated. The properties of the phase space and the physically relevant solutions will be examined to explore the behaviour of the rolling wheelset proposed by this physical model.

Chapter 3

Analysis of the equation of motion

3.1 Analysis of the system of equations

Our investigation starts from equations (2.3.59)-(2.3.62), let $Y : (x, \varphi, \psi, \vartheta) \to (\dot{x}, \dot{\varphi}, \dot{\psi}, \dot{\vartheta})$ denote the four dimensional vector field generated by them.

As one can quickly recognise this vector field does not depend on φ and x, which has an obvious physical explanation. The independence from φ is caused by the axysymmetry of the wheelset, and change of x has also no effect, because the system is symmetric with respect to translation of the wheelset along the track.

Hence x and φ can be separated from the system, because the dynamics of ϑ and ψ can be determined without these so-called cyclic coordinates. Let us denote the restricted vector field by $X : (\psi, \vartheta) \to (\dot{\psi}, \dot{\vartheta})$, where the components of X are generated by (2.3.61)-(2.3.62):

$$X_1(\psi, \vartheta) = -\sin\vartheta \cdot S(\psi, \vartheta) \tag{3.1.1}$$

$$X_2(\psi, \vartheta) = \frac{h^2 \sin\psi}{1 - h^2 \tan^2\psi} \left(k - \frac{\cos\vartheta \cos\psi - l}{\cos^2\psi} \right) \cdot S(\psi, \vartheta) \tag{3.1.2}$$

The range of the two variables of X can be taken to $\psi \in (-\pi/2, \pi/2)$ and $\vartheta \in [-\pi, \pi)$. The singularity of the Euler parametrisation at $\psi = \pm\pi/2$ does not cause a problem, because such large yaw angles are physically unavailable. Thus the phase space is:

$$U := (-\pi/2, \pi/2) \times [-\pi, \pi) \subset \mathbb{R}^2 \tag{3.1.3}$$

An element from the space is denoted by pairs $(\psi, \vartheta) \in U$, and $X = (X_1, X_2)$ is a $U \to \mathbb{R}^2$, function which may have singularities on U.

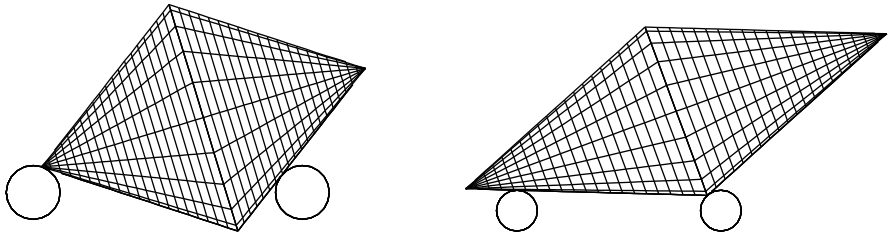

Figure 3.1: The restrictions caused by the apex (left) and the base circle (right). These cases are not available by real wheelsets due to the flanges, but conditions of them mean a sufficient condition to exclude some problematic parts of the phase plane explicitly.

Therefore the system of X can be written as

$$\begin{aligned} \dot{\psi} &= X_1(\psi, \vartheta) \\ \dot{\vartheta} &= X_2(\psi, \vartheta) \end{aligned} \tag{3.1.4}$$

which a set of two first-order autonomous differential equations.

The system (3.1.4) has a trivial fixed point at the origin. If this is substituted into Y, we get the following solution:

$$x = x_0 + vt \qquad \varphi = \varphi_0 + \frac{v}{dh(k-1+l)}t \qquad \psi \equiv 0 \qquad \vartheta \equiv 0 \tag{3.1.5}$$

This is called a stationary solution of Y, which refers to the natural motion of the wheelset, the hunting caused by ψ and ϑ is not present. Thus the investigation of the stationary motion (3.1.5) of Y can be performed by examining the fixed point of X in the origin, which is done in the following subsections.

3.1.1 Physical restrictions of the bicone

During the derivation of the equation of motion we have found a strict condition in (2.3.15) which corresponds to the possibility of the tangent constraint, but we did not take into consideration the permitted range of the surface parameters of the contact points. These are determined by (2.2.21), (2.2.24) and (2.3.13). Investigation of these conditions helps to find and analyse only the physically relevant areas of U.

Practically we find restrictions only for χ^l and χ^r, which is caused by the finite height of the bicone. The contact points can pass neither through the apex of the cone, nor through the base circle of the bicone (condition (2.3.13)). Let us call these properties *apex effect* and *base circle effect*. The explanation can be seen in Figure 3.1.

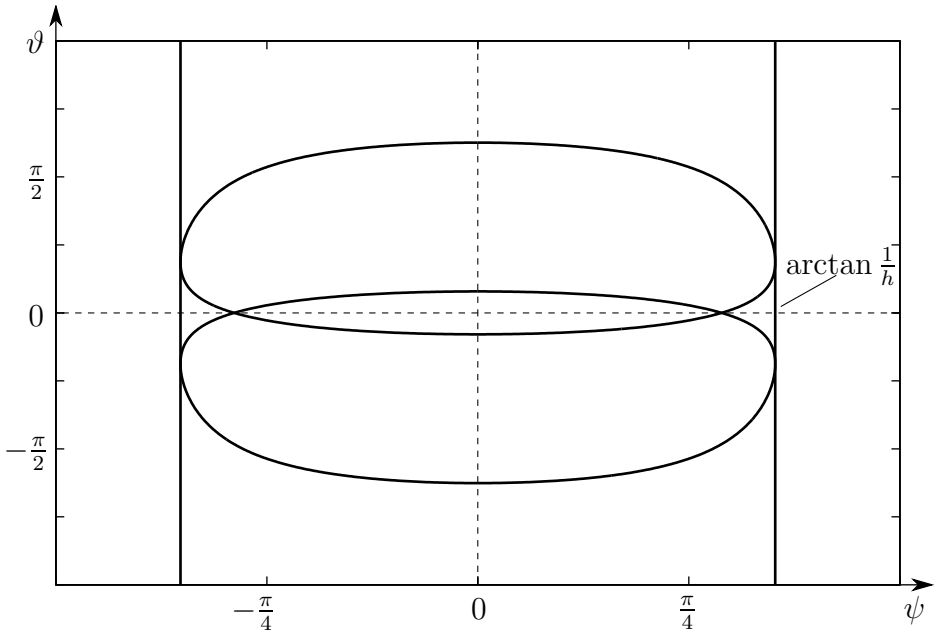

Figure 3.2: Restriction curves of the apex effect, $h = 0.5, k = 1.36, l = 0.1$. The vertical straight lines correspond to the requirement of non-negative expression under the square root in (3.1.6), which coincides with (2.3.15).

The apex effect is ensured by first row of (2.2.24). If χ^l and χ^r expressed from (2.3.30) and (2.3.31) are substituted into that we get:

$$\pm \sin\vartheta \cos^2\psi \sqrt{1 - h^2 \tan^2\psi} + kh \cos^2\psi - h(\cos\vartheta \cos\psi - l) > 0 \tag{3.1.6}$$

The boundary curves in explicit form is:

$$\vartheta(\psi) = \pm \arccos \frac{h(k\cos^2\psi + l)}{\cos^2\psi\sqrt{1+h^2}} \pm \arccos \frac{h}{\cos\psi\sqrt{1+h^2}} \tag{3.1.7}$$

These typical curves on the phase plane can be observed in figure 3.2, the effect of the parameters on the curves and the allowed regions can be seen in figure 3.3.

The base circle effect is ensured by restrictions in (2.3.13). Substituting them into (2.3.30) and (2.3.31) we obtain:

$$\pm \sin\vartheta \cos^2\psi \sqrt{1 - h^2 \tan^2\psi} + kh^3 \sin^2\psi - h(\cos\vartheta \cos\psi - l) < 0 \tag{3.1.8}$$

The boundary curves explicitly:

$$\vartheta(\psi) = \pm \arccos \frac{h(kh^2\sin^2\psi + l)}{\cos^2\psi\sqrt{1+h^2}} \pm \arccos \frac{h}{\cos\psi\sqrt{1+h^2}} \tag{3.1.9}$$

These curves can be seen in Figure 3.4, and the parametric dependence in Figure 3.5. For determining the allowed region, the intersect of gray areas of Figures 3.3 and 3.5 can be considered.

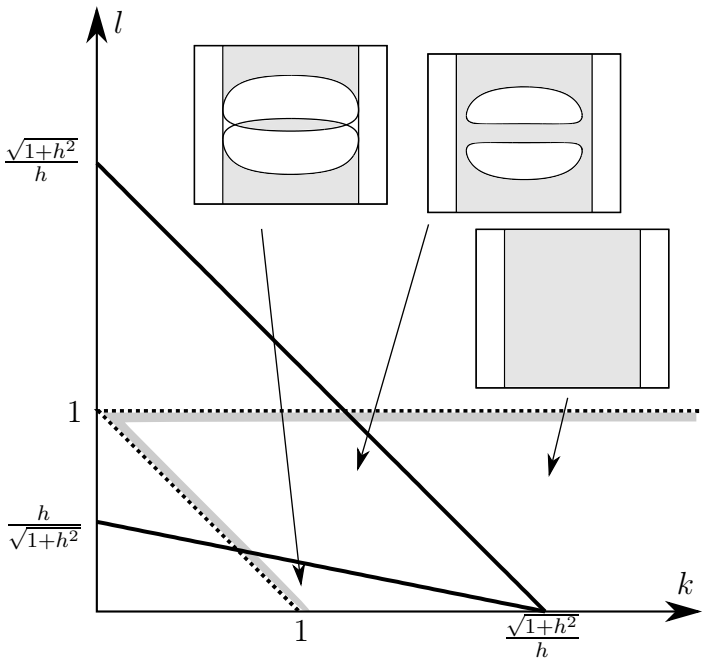

Figure 3.3: Regions allowed by the apex effect - dependence on parameters. The continuous thick lines denote the boundary between the topologically different regions. The small diagrams have the small meaning as Figure 3.2. The dotted line with the gray stripe denote the region of physically relevant region determined by the positiveness of $1-l$ and $k-1+l$ according to Figure 2.10

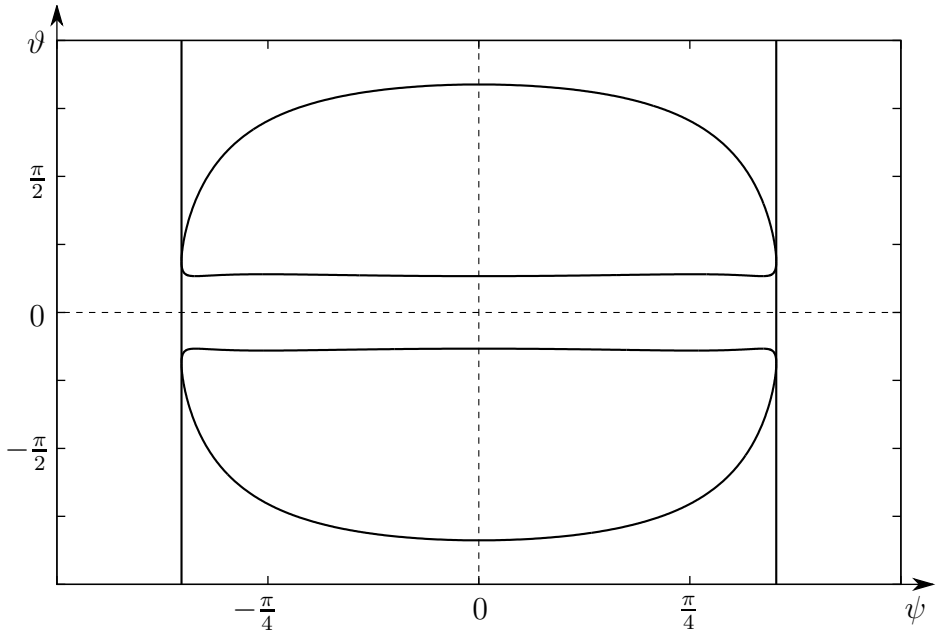

Figure 3.4: Restriction curves of the base circle effect, $h = 0.5, k = 1.36, l = 0.1$. The vertical straight lines are the same as in Figure 3.2.

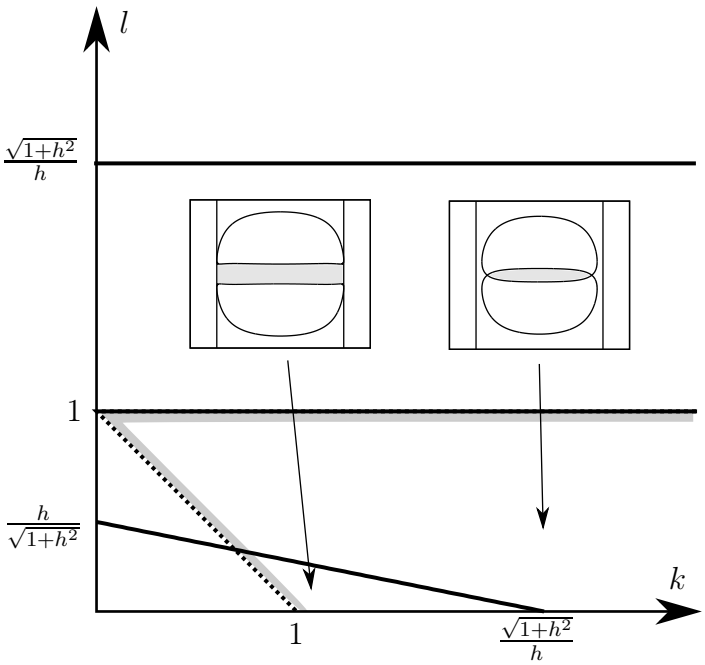

Figure 3.5: Regions allowed by the base circle effect - dependence on parameters. Notations are the same as in Figure 3.3.

3.1.2 Singularities

Now the singularities of (3.1.4) are determined, where the vector field is not defined. The X_2 function is singular on the curve

$$1 - h^2 \tan^2 \psi = 0 \tag{3.1.10}$$

On this boundary X_1 is generally finite, therefore trajectories approaching this curve tend to the vertical direction on the phase plane.

Another singularity occurs when the denominator of the fraction of $S(\psi, \vartheta)$ in (2.3.63) is zero, that is:

$$\frac{\cos\vartheta\cos\psi - l}{\cos^2\psi}\left(k - \frac{\cos\vartheta\cos\psi - l}{\cos^2\psi}\right)h^2 + \sin^2\vartheta(1 - h^2\tan^2\psi) = 0 \tag{3.1.11}$$

This can be reformulated to a second-order equation, and $\cos\vartheta$ can be expressed explicitly, but the formula is complicated.

Conditions of singularities fulfil only for relatively large ψ and ϑ angles, which are outside of our interest. It can be showed already from the implicit form of the curves, that (3.1.10) and (3.1.11) does not intersect the area determined by (3.1.6) and (3.1.8). The singular curves can be seen in Figures 3.6 and 3.7 for some example values.

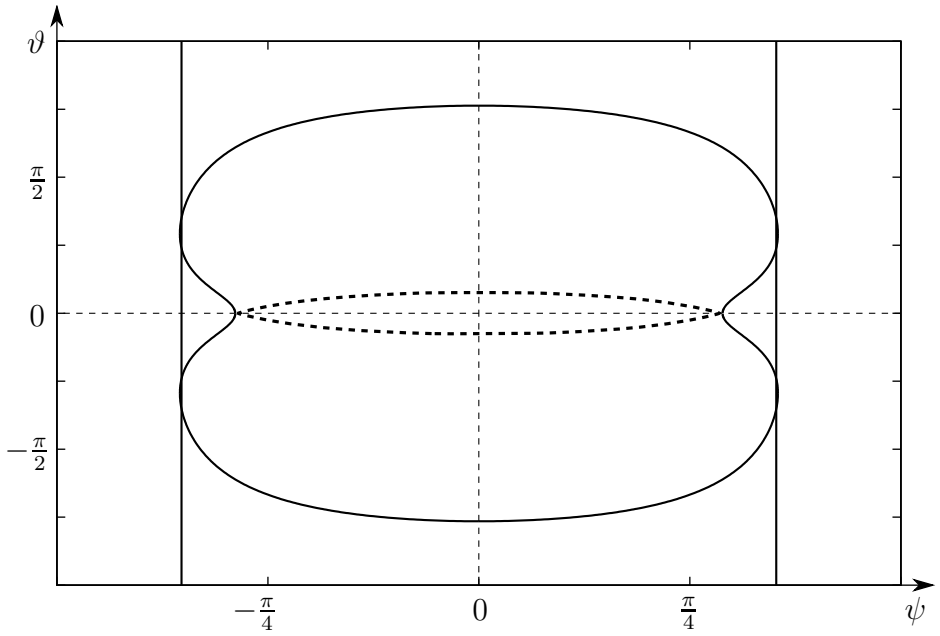

Figure 3.6: Singular curves on the phase plane, $h = 0.5, k = 1.36, l = 0.1$, the dashed line denotes area denotes the allowed region due to physical restrictions. In this case the singular curve goes through the edge of the boundary of this area.

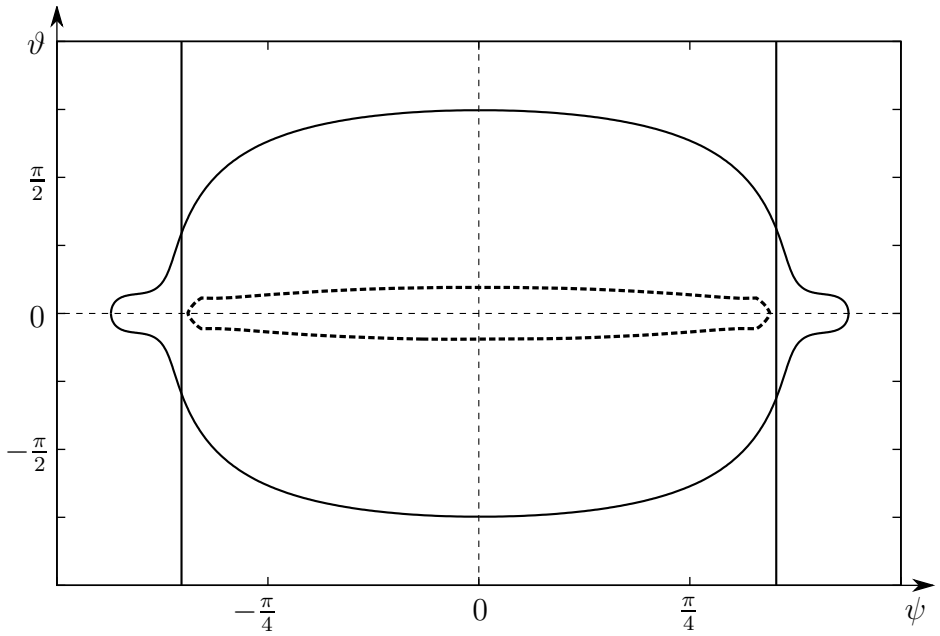

Figure 3.7: Singular curves on the phase plane, $h = 0.5, k = 1.36, l = 0.2$, the dashed line denotes area denotes the allowed region due to physical restrictions. In this case the singular curves are not in connection with this area.

3.1.3 Linear stability of the origin

Let us determine the fixed points of the system (3.1.4). First the nullclines are calculated, that is, the curves where X_1 or X_2 are zero:

$$X_1(\psi,\vartheta)=0 \quad \Leftrightarrow \quad \begin{array}{c} \sin\vartheta=0 \\ \text{or} \\ \cos\psi=0 \end{array} \tag{3.1.12}$$

$$X_2(\psi,\vartheta)=0 \quad \Leftrightarrow \quad \begin{array}{c} \sin\psi=0 \\ \text{or} \\ \cos\psi=0 \\ \text{or} \\ k-\frac{\cos\vartheta\cos\psi-l}{\cos^2\psi}=0 \end{array} \tag{3.1.13}$$

As $\psi\in(-\pi/2,\pi/2)$, the $\cos\psi=0$ condition could not be fulfilled. From these the candidates for being fixed points are:

$$\begin{aligned} (\psi_1,\vartheta_1)&=(0,0)\\ (\psi_2,\vartheta_2)&=(0,-\pi)\\ (\psi_{3,4},\vartheta_{3,4})&=\left(\arccos\frac{1\pm\sqrt{1-4kl}}{2k},0\right) \end{aligned} \tag{3.1.14}$$

Points (ψ_3,ϑ_3) and (ψ_4,ϑ_4) are on the singularity curve (3.1.11), and calculating the limits they prove singular points. Point $(-\pi,0)$ is surely out of the range of both (3.1.6) and (3.1.8), which is physically meaningless. Therefore the origin is the only fixed point, which corresponds to the physical reality.

As we found in (3.1.5), $(0,0)$ corresponds to the natural motion of the wheelset. The linear approximation of the system field around the origin is:

$$\begin{aligned} \dot\psi&=a_{10}\psi+a_{01}\vartheta+\mathcal{O}^2(\psi,\vartheta)\\ \dot\vartheta&=b_{10}\psi+b_{01}\vartheta+\mathcal{O}^2(\psi,\vartheta), \end{aligned} \tag{3.1.15}$$

where the coefficients are:

$$\begin{aligned} a_{10}&:=\partial_1X_1(0,0)=0\\ a_{01}&:=\partial_2X_1(0,0)=\frac{-V}{h^2(1-l)(k-1+l)}\\ b_{10}&:=\partial_1X_2(0,0)=\frac{V}{1-l}\\ b_{01}&:=\partial_2X_2(0,0)=0 \end{aligned} \tag{3.1.16}$$

Therefore the linear approximation in matrix form is:

$$\begin{bmatrix} \dot{\psi} \\ \dot{\vartheta} \end{bmatrix} = \begin{bmatrix} 0 & \frac{-V}{h^2(1-l)(k-1+l)} \\ \frac{V}{1-l} & 0 \end{bmatrix} \begin{bmatrix} \psi \\ \vartheta \end{bmatrix} + \mathcal{O}^2(\psi, \vartheta) \tag{3.1.17}$$

The characteristic equation of the matrix is:

$$\lambda^2 + \frac{V^2}{h^2(1-l)^2(k-1+l)} = 0 \tag{3.1.18}$$

It can be seen from Figure 2.10, that in the physically relevant case $k-1+l > 0$ and $1-l > 0$. Then the eigenvalues of the system are $\pm i\omega$, where i is the imaginary unit, and

$$\omega := \sqrt{a_{01}b_{10}} = \frac{V}{h(1-l)\sqrt{k-1+l}} \tag{3.1.19}$$

Or, with the original parameters:

$$\boxed{\omega = \frac{v}{d - \frac{rh}{\sqrt{1+h^2}}} \sqrt{\frac{hd}{R - h\left(d - \frac{rh}{\sqrt{1+h^2}}\right)}}} \tag{3.1.20}$$

If we introduce the effective half-distance

$$\hat{d} := d - \frac{rh}{\sqrt{1+h^2}} \tag{3.1.21}$$

and the effective radius

$$\hat{R} := R - h\left(d - \frac{rh}{\sqrt{1+h^2}}\right), \tag{3.1.22}$$

we get

$$\omega = \frac{v}{\hat{d}}\sqrt{\frac{hd}{\hat{R}}}, \tag{3.1.23}$$

which is the same as Lorant's result in (1.2.3).

The origin of the linear system is a centre, but this is not surely true for the nonlinear equation. Hence nonlinear techniques are needed for determining the orbit structure around the origin.

3.1.4 Nonlinear stability of the origin

The Hopf Bifurcation Theorem can be used to determine the type of a fixed point, which is a centre in the linear approximation of the system. Let us continue the Taylor expansion of (3.1.15) up to the third-order terms:

$$\begin{aligned} \dot{\psi} &= a_{01}\vartheta + a_{03}\vartheta^3 + a_{21}\vartheta\psi^2 + \mathcal{O}^4(\psi, \vartheta) \\ \dot{\vartheta} &= b_{10}\psi + b_{30}\psi^3 + b_{12}\psi\vartheta^2 + \mathcal{O}^4(\psi, \vartheta), \end{aligned} \tag{3.1.24}$$

where

$$a_{ij} := \frac{1}{i!j!}\partial_1^i \partial_2^j X_1(0,0) \tag{3.1.25}$$

$$b_{ij} := \frac{1}{i!j!}\partial_1^i \partial_2^j X_2(0,0) \tag{3.1.26}$$

and the coefficients equal to zero are omitted from (3.1.24).

With an appropriate linear transformation the first-order normal form can be calculated. Let

$$\begin{bmatrix}\tilde{\psi}\\ \tilde{\vartheta}\end{bmatrix} := \begin{bmatrix}\sqrt{\frac{\omega}{-a_{01}}} & 0\\ 0 & \sqrt{\frac{\omega}{b_{10}}}\end{bmatrix}\begin{bmatrix}\psi\\ \vartheta\end{bmatrix} \tag{3.1.27}$$

Applying the transformation, the linear normal form of 3.1.24 is obtained:

$$\begin{bmatrix}\dot{\tilde{\psi}}\\ \dot{\tilde{\vartheta}}\end{bmatrix} = \begin{bmatrix}0 & -\omega\\ \omega & 0\end{bmatrix}\begin{bmatrix}\tilde{\psi}\\ \tilde{\vartheta}\end{bmatrix} + \begin{bmatrix}\tilde{a}_{03}\tilde{\vartheta}^3 + \tilde{a}_{21}\tilde{\vartheta}\tilde{\psi}^2 + \mathcal{O}^4(\tilde{\psi},\tilde{\vartheta})\\ \tilde{b}_{30}\tilde{\psi}^3 + \tilde{b}_{12}\tilde{\psi}\tilde{\vartheta}^2 + \mathcal{O}^4(\tilde{\psi},\tilde{\vartheta})\end{bmatrix} \tag{3.1.28}$$

The new coefficients with the tilde can be calculated from the transformation. Let us calculate the Poincare-Lyapunov constant δ (according to the book of Wiggins [18], p. 385):

$$\begin{aligned}\delta = \frac{1}{16}(\tilde{a}_{30} + \tilde{a}_{12} + \tilde{b}_{21} + \tilde{b}_{03}) + \\ + \frac{1}{16\omega}\left(\tilde{a}_{11}(\tilde{a}_{20} + \tilde{a}_{02}) - \tilde{b}_{11}(\tilde{b}_{20} + \tilde{b}_{02}) - \tilde{a}_{20}\tilde{b}_{20} + \tilde{a}_{02}\tilde{b}_{02}\right)\end{aligned} \tag{3.1.29}$$

All coefficients which are needed for the formula are missing from (3.1.28), therefore the Poincare-Lyapunov constant is identically zero. If it were positive or negative, the fixed point would be found to be an unstable or stable focus, respectively. But in the case of $\delta = 0$ the Hopf Bifurcation Theorem cannot help to determine the stability, the fixed point can be either a centre or a focus.

However the answer can be obtained by exploiting the symmetries of X. The vector field X on a set U is called *(time-)reverse symmetric* with respect to an invertible mapping G of U onto itself, if

$$(\mathrm{D}G)X + X \circ G = 0 \tag{3.1.30}$$

where DG is the Jacobian tensor of G, and $\circ$ refers composition of functions. This definition means that if we apply the transformation G on the phase space, then the orbits of the system of X remain the same, only the direction of the time is reversed. If G is a time-reverse symmetry of the system, then it preserves the curves of the trajectories.

We can found two simple, linear symmetries for our system (3.1.4), denoted by $G = (G_1, G_2)$ and $F = (F_1, F_2)$:

$$\begin{aligned} G_1(\psi, \vartheta) &:= \psi \\ G_2(\psi, \vartheta) &:= -\vartheta \end{aligned} \tag{3.1.31}$$

This transformation G performs a mirroring respect to the axis ψ. This symmetry can be checked if we substitute it to the definition (3.1.30):

$$\begin{aligned} X_1(\psi, \vartheta) + X_1(\psi, -\vartheta) &= 0 \\ -X_2(\psi, \vartheta) + X_2(\psi, -\vartheta) &= 0 \end{aligned} \tag{3.1.32}$$

Therefore X_1 must be an odd, and X_2 to be an even function of ϑ, which is true.

The other, similar reverse-symmetric transformation is:

$$\begin{aligned} F_1(\psi, \vartheta) &:= -\psi \\ F_2(\psi, \vartheta) &:= \vartheta \end{aligned} \tag{3.1.33}$$

This means a mirroring to the $\vartheta = 0$ axis. Substituting it back to (3.1.30):

$$\begin{aligned} -X_1(\psi, \vartheta) + X_1(-\psi, \vartheta) &= 0 \\ X_2(\psi, \vartheta) + X_2(-\psi, \vartheta) &= 0 \end{aligned} \tag{3.1.34}$$

The meaning of this condition is that X_1 is even, and X_2 is an odd function of ψ, which can be checked from the formulae of these functions.

These symmetries cause that the trajectories on the phase space are symmetric with respect to the two axes of the coordinate system which is true also for the orbits around the origin. It can be our strong corollary, that in the close neighbourhood of a focus, the orbits cannot be symmetric to the axes, therefore the origin should be a centre.

Although this statement is not obvious, it can be proved. We can state (book of Strogatz [16], p. 164), that if only one of the mirroring time-reverse symmetries G and F is present in the system, and the origin of the linear system is a centre, then the origin of the nonlinear system is also a centre.

In other words, there is a neighbourhood around the origin of (3.1.4)*, within which all trajectories are closed. Therefore the origin of X is a centre, which is neutrally stable.*

It is an interesting question if the system in (3.1.4) is conservative or not, or in other words, if there is a function of the state variables which is preserved along

the trajectories. It is known from basic examples, that a time-reverse symmetric system can be both conservative and non-conservative.

The question of conservativity is not examined here, but in some sense we can say, that the system is *locally conservative* around the origin. That is, an energy function can be constructed by using the closed trajectories as level sets, which is constant along the orbits.

This conservative region can be extended surely as far as the trajectories are closed. The investigation of the extent and the boundary of this area is not examined in this project, it can be a further task.

3.2 Transformation to a second-order equation

Every second-order differential equation can be transformed to a two-dimensional system of first-order equations, which is done regularly during investigation of the one degree-of-freedom mechanical systems. Our situation is the opposite, we already have the system in (3.1.4), but after finding a second-order equation equivalent to the system, we can understand the equation better by exploiting the methods and formalisms of mechanics.

It seems to be hopeless to do it analytically with our system (3.1.4). However after an appropriate change of the time variable, a fully nonlinear second-order equation can be calculated. After that a local, approximate equation is presented, for making quantitative analysis easier.

3.2.1 Exact transformation using the new time variable

Let us first extend the system (3.1.4) with a third state variable, τ. Let us suppose, that τ is a cyclic coordinate, therefore it does not have an effect on the dynamics any of the variables. Thus X_1 and X_2 functions are preserved, and the third component of the extended vector field is defined, denoted by X_3:

$$\dot{\tau} = X_3(\psi, \vartheta) := S(\psi, \vartheta) \tag{3.2.1}$$

From ψ, ϑ, τ and X_1, X_2, X_3 a three dimensional dynamical system is composed, which provides the same solutions for ψ and ϑ as (3.1.4).

Now let us differentiate ψ and ϑ with respect to τ, using the chain rule:

$$\frac{\mathrm{d}\psi}{\mathrm{d}\tau} = \frac{\dot{\psi}}{\dot{\tau}} = \frac{X_1}{X_3} = -\sin\vartheta \tag{3.2.2}$$

$$\frac{\mathrm{d}\vartheta}{\mathrm{d}\tau} = \frac{\dot{\vartheta}}{\dot{\tau}} = \frac{X_1}{X_3} = \frac{h^2 \sin\psi}{1 - h^2 \tan^2\psi}\left(k - \frac{\cos\vartheta\cos\psi - l}{\cos^2\psi}\right) \tag{3.2.3}$$

This two equations build a new dynamical system, and it can be solved for the functions $\tilde{\vartheta}(\tau)$ and $\tilde{\psi}(\tau)$. The tilde sign is omitted in the following calculations, if it is unnecessary, but the derivative respect to τ is denoted by accents instead of dots.

Therefore the following system of equations are obtained:

$$\begin{aligned} \psi' &= Z_1(\vartheta, \psi) \\ \vartheta' &= Z_2(\vartheta, \psi) \end{aligned} \tag{3.2.4}$$

where

$$Z_1(\psi, \vartheta) := -\sin\vartheta \tag{3.2.5}$$

$$Z_2(\psi, \vartheta) := \frac{h^2 \sin\psi}{1 - h^2 \tan^2\psi}\left(k - \frac{\cos\vartheta\cos\psi - l}{\cos^2\psi}\right) \tag{3.2.6}$$

In fact, a transformation on the independent time variable has been done from t to τ, but this transformation is defined by the dependent variables ψ and ϑ. This leads a complication when one tries to calculate for example the $\vartheta(t)$ function from $\vartheta(\tau)$ obtained from (3.2.4). However the tangent of the trajectories $\mathrm{d}\vartheta/\mathrm{d}\psi$ remain the same, thus the trajectories can be examined using (3.2.4) instead of (3.1.4).

With (3.2.4) a much simpler form of the equations are obtained, from which a second-order equation can be created for ψ. From (3.2.5) the sine of ϑ can be expressed:

$$\sin\vartheta = -\psi' \tag{3.2.7}$$

The cosine of ϑ:

$$\cos\vartheta = \sqrt{1 - \psi'^2} \tag{3.2.8}$$

Differentiating (3.2.7):

$$\psi'' = -\cos\vartheta\,\vartheta' \tag{3.2.9}$$

The expression for ϑ' can be obtained from (3.2.6), and after eliminating all ϑ-dependent terms by using (3.2.7)-(3.2.8) the second-order equation is obtained:

$$\boxed{\psi'' + \sqrt{1 - \psi'^2}\frac{h^2 \sin\psi}{1 - h^2 \tan^2\psi}\left(k - \frac{\sqrt{1 - \psi'^2}\cos\psi - l}{\cos^2\psi}\right) = 0} \tag{3.2.10}$$

Solving that for $\tilde{\psi}(\tau)$ and calculating $\tilde{\vartheta}(\tau) = -\arcsin\tilde{\psi}'(\tau)$ the same trajectories can be obtained as for (3.1.4). However the complicated singularity of $S(\psi, \vartheta)$ is eliminated in (3.2.4) and (3.2.10). Therefore the phase portrait can be illustrated easier using a numerical simulation. (Figures 3.8-3.9).

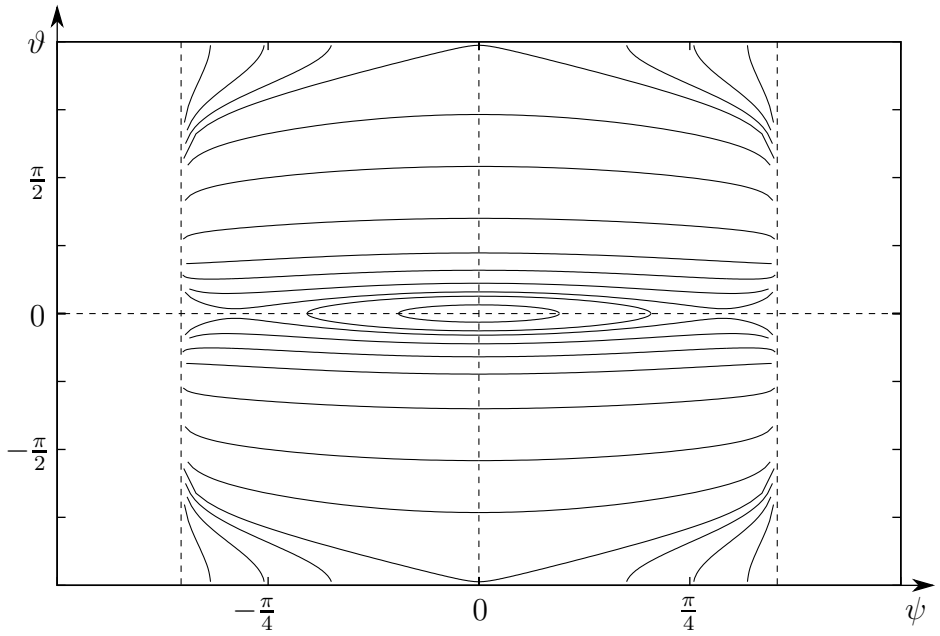

Figure 3.8: Phase portrait of the system by numerical simulation, $h = 0.5, k = 1.36, l = 0.1$. It is made by fourth-order Runge-Kutta method used on (3.2.4). In the case of (3.2.4), there are two saddle points on the ψ axis, which are the same as in the third row of (3.1.14). Although these saddles are eliminated in the original equation (3.1.4) by the singularities, the orbit structure remains the same.

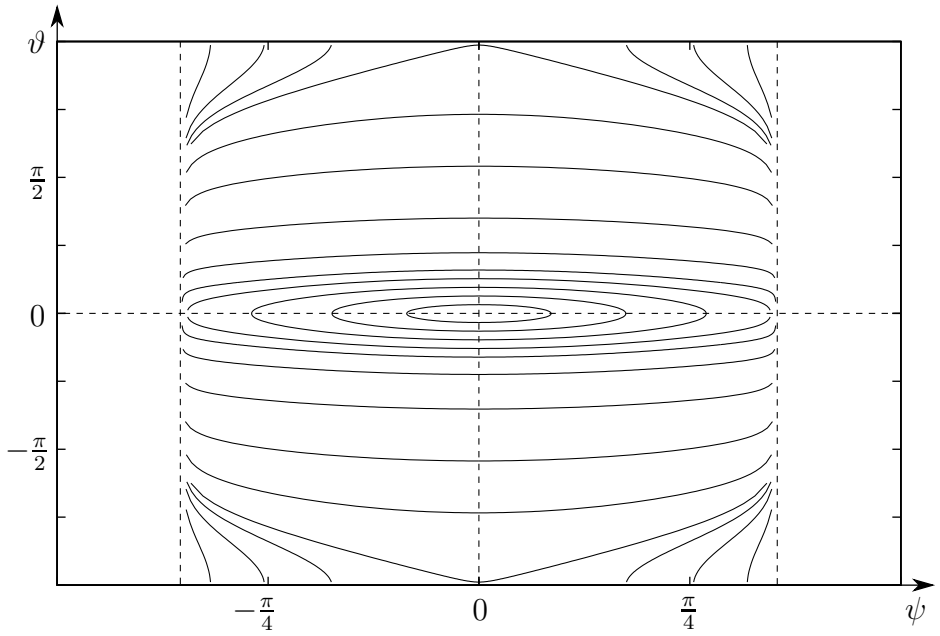

Figure 3.9: Phase portrait of the system by numerical simulation, $h = 0.5, k = 1.36, l = 0.2$. Increasing the value of l in Figure 3.8, the saddle points reach the singular lines, and the orbit stucture changes. The bifurcation points can be calculated from the third row of (3.1.14).

3.2.2 Approximation with the original time variable

If quantitative information is also needed about movement on the trajectories, the original time variable should be used. The method used for (3.2.4) leads so complicated formulae if we apply it for (3.1.4), that no analytical results can be obtained. Therefore we derive a nonlinear approximation of the second-order equation.

The first equation of (3.1.4) means an $(\psi, \vartheta) \to \dot{\psi}$ mapping. The inverse function $(\psi, \dot{\psi}) \to \vartheta$ should be calculated to eliminate ϑ. This process can be done up to the third-order terms applying implicit differentiation on the first equation of (3.1.24):

$$\vartheta = \frac{1}{a_{01}}\dot{\psi} - \frac{a_{03}}{a_{01}^4}\dot{\psi}^3 - \frac{a_{21}}{a_{01}^2}\dot{\psi}\psi^2 + \mathcal{O}^5(\psi, \dot{\psi}) \tag{3.2.11}$$

Let us now differentiate the first equation of (3.1.24) with respect to time:

$$\ddot{\psi} = a_{01}\dot{\vartheta} + 3a_{03}\vartheta^2\dot{\vartheta} + a_{21}\dot{\vartheta}\psi^2 + 2a_{21}\vartheta\psi\dot{\psi} + \mathcal{O}^5(\vartheta, \dot{\vartheta}, \psi, \dot{\psi}) \tag{3.2.12}$$

Let us substitute the second equation of (3.1.24) into this:

$$\ddot{\psi} = a_{01}b_{10}\psi + a_{01}b_{30}\psi^3 + a_{01}b_{12}\psi\vartheta^2 + 3a_{03}b_{10}\vartheta^2\psi + a_{21}b_{10}\psi^3 + \\ + 2a_{21}\vartheta\psi\dot{\psi} + \mathcal{O}^5(\vartheta, \psi, \dot{\psi}) \tag{3.2.13}$$

The function from (3.2.11) is also substituted:

$$\ddot{\psi} = a_{01}b_{10}\psi + a_{01}b_{30}\psi^3 + \frac{b_{12}}{a_{01}}\psi\dot{\psi}^2 + \frac{3a_{03}b_{10}}{a_{01}^2}\psi\dot{\psi}^2 + a_{21}b_{10}\psi^3 + \\ + \frac{2a_{21}}{a_{01}}\psi\dot{\psi}^2 + \mathcal{O}^5(\psi, \dot{\psi}) \tag{3.2.14}$$

After collecting the terms of the variables:

$$\ddot{\psi} = a_{01}b_{10}\psi + (a_{01}b_{30} + a_{21}b_{10})\,\psi^3 + \left(\frac{b_{12}}{a_{01}} + \frac{3a_{03}b_{10}}{a_{01}^2} + \frac{2a_{21}}{a_{01}}\right)\psi\dot{\psi}^2 + \mathcal{O}^5(\psi, \dot{\psi}) \tag{3.2.15}$$

New constants can be introduced:

$$\begin{aligned} \omega^2 &:= -a_{01}b_{10} \\ \mu &:= -\left(a_{01}b_{30} + a_{21}b_{10}\right) \\ \nu &:= -\left(\frac{b_{12}}{a_{01}} + \frac{3a_{03}b_{10}}{a_{01}^2} + \frac{2a_{21}}{a_{01}}\right) \end{aligned} \tag{3.2.16}$$

The notation ω forecasts, that it is equal to (3.1.19). With these, (3.2.15) becomes:

$$\boxed{\ddot{\psi} + \omega^2\psi + \mu\psi^3 + \nu\psi\dot{\psi}^2 + \mathcal{O}^5(\psi, \dot{\psi}) = 0} \tag{3.2.17}$$

which can be used as a third-order approximation of the second-order equation for ψ.

3.2.3 Approximation with the new time variable

A third-order equation similar to (3.2.17) can be obtained from the equation (3.2.10). Let:

$$W(\psi,\psi') := \sqrt{1-\psi'^2}\frac{h^2\sin\psi}{1-h^2\tan^2\psi}\left(k-\frac{\sqrt{1-\psi'^2}\cos\psi-l}{\cos^2\psi}\right) \tag{3.2.18}$$

With this, (3.2.10) becomes

$$\psi'' + W(\psi,\psi') = 0 \tag{3.2.19}$$

Calculating the Taylor expansion respect to the variables ψ and ψ':

$$\boxed{\psi'' + \bar{\omega}^2\psi + \bar{\mu}\psi^3 + \bar{\nu}\psi\psi'^2 + \mathcal{O}^5(\psi,\psi') = 0} \tag{3.2.20}$$

where

$$\begin{aligned}\bar{\omega}^2 &:= \partial_1 W(0,0)\\ \bar{\mu} &:= \partial_1^3 W(0,0)\\ \bar{\nu} &:= \partial_1\partial_2^2 W(0,0)\end{aligned} \tag{3.2.21}$$

Equation (3.2.20) can be examined in the same way as (3.2.17), but the constants of them are obviously not the same. The connection between them can be derived through the transformation (3.2.2). The derivatives with respect to τ can be expressed with time derivatives according to the definition:

$$\begin{aligned}\psi'' &= \frac{\ddot{\psi}}{\dot{\tau}^2}\\ \psi' &= \frac{\dot{\psi}}{\dot{\tau}}\end{aligned} \tag{3.2.22}$$

Substituting them back to (3.2.20):

$$\frac{\ddot{\psi}}{\dot{\tau}^2} + \bar{\omega}^2\psi + \bar{\mu}\psi^3 + \bar{\nu}\psi\left(\frac{\dot{\psi}}{\dot{\tau}}\right)^2 + \mathcal{O}^5\left(\psi,\frac{\dot{\psi}}{\dot{\tau}}\right) = 0 \tag{3.2.23}$$

Multiplying by $\dot{\tau}^2$:

$$\ddot{\psi} + \bar{\omega}^2\psi\dot{\tau}^2 + \bar{\mu}\psi^3\dot{\tau}^2 + \bar{\nu}\psi\dot{\psi}^2 + \dot{\tau}^2\mathcal{O}^5\left(\psi,\frac{\dot{\psi}}{\dot{\tau}}\right) = 0 \tag{3.2.24}$$

Let us expand $\dot{\tau}^2$ into Taylor series:

$$\dot{\tau}^2 = X_3^2(\psi,\vartheta) = c_{00} + c_{20}\psi^2 + c_{02}\vartheta^2 + \mathcal{O}^2(\psi^2,\vartheta^2), \tag{3.2.25}$$

where

$$\begin{aligned} c_{00} &:= X_3^2(0,0) \\ c_{20} &:= \partial_1^2 X_3^2(0,0) \\ c_{02} &:= \partial_2^2 X_3^2(0,0) \end{aligned} \tag{3.2.26}$$

The term ϑ^2 can be expressed using (3.2.7):

$$\vartheta^2 = \psi'^2 + \mathcal{O}^2(\psi'^2) = \frac{\dot{\psi}^2}{\dot{\tau}^2} + \mathcal{O}^2\left(\frac{\dot{\psi}^2}{\dot{\tau}^2}\right) \tag{3.2.27}$$

After implicit differentiation and substitution to (3.2.25):

$$\dot{\tau}^2 = c_{00} + c_{20}\psi^2 + \frac{c_{02}}{c_{00}}\dot{\psi}^2 + \mathcal{O}^2(\psi^2, \dot{\psi}^2) \tag{3.2.28}$$

Finally after substituting to (3.2.24) we get:

$$\ddot{\psi} + \left(\bar{\omega}^2 c_{00}\right)\psi + \left(\bar{\mu}c_{00} + \bar{\omega}^2 c_{20}\right)\psi^3 + \left(\bar{\nu} + \bar{\omega}^2\frac{c_{02}}{c_{00}}\right)\psi\dot{\psi}^2 + \mathcal{O}^5(\psi, \dot{\psi}) = 0 \tag{3.2.29}$$

Comparing to (3.2.17) the constants are:

$$\begin{aligned} \omega^2 &= \bar{\omega}^2 c_{00} \\ \mu &= \bar{\mu}c_{00} + \bar{\omega}^2 c_{02} \\ \nu &= \bar{\nu} + \bar{\omega}^2\frac{c_{20}}{c_{00}} \end{aligned} \tag{3.2.30}$$

This means an alternative method to (3.2.16) to determine ω^2, μ and ν.

3.2.4 Calculating the parameters of the approximation

Equation (3.2.17) can be obtained directly or through (3.2.20). It is useful to produce the constants using the physical parameters of the mechanical system. The linear coefficient is known from (3.1.19):

$$\omega^2 = \frac{v^2 hd}{\left(d - \frac{rh}{\sqrt{1+h^2}}\right)^2 \left(R - h\left(d - \frac{rh}{\sqrt{1+h^2}}\right)\right)} \tag{3.2.31}$$

Similar, but much longer expressions can be calculated for μ and ν using (3.2.16) or (3.2.30), which are not presented here. But if h is small, these expressions can be expanded to Taylor series respect to h. With the original parameters:

$$\frac{\mu}{\omega^2} = -\frac{7}{6} - \frac{4rR + 2d^2}{3Rd}h + \mathcal{O}^2(h) \tag{3.2.32}$$

$$\nu = -3 + \frac{3R^2 - 10rR - 2d^2}{2Rd}h + \mathcal{O}^2(h) \tag{3.2.33}$$

For small h, the leading approximations $\mu \approx -7/6$ and $\nu \approx -3$ can be used effectively.

3.3 Analysis of the third-order approximation

Let us investigate the behaviour of the system around the origin. Then the fifth-order terms in (3.2.17) can be neglected and the following approximate equation is obtained:

$$\ddot{\psi} + \omega^2\psi + \mu\psi^3 + \nu\psi\dot{\psi}^2 = 0 \tag{3.3.1}$$

In many nonlinear dynamics books a similar equation, namely the undamped Duffing oscillator is investigated, which can be obtained from (3.3.1) substituting $\nu = 0$. That is probably the simplest equation which is appropriate to demonstrate the differences between linear and nonlinear systems. However the behaviour of (3.3.1) is examined now, focused on effect of the ν parameter.

3.3.1 Iterative method of finding an energy function

It has been obtained at Subsection 3.1.4, that the orbits around the origin constitutes a nonlinear centre, and there exists an energy function in the neighbourhood of the centre. As the symmetries of (3.1.24) are preserved in (3.3.1), thus the existence of the energy function can be expected, at least locally. Let us try to calculate this energy function.

For the shorter notation the terms in the equation depending on only ψ are collected:

$$f(\psi) := \omega^2\psi + \mu\psi^3 \tag{3.3.2}$$

The following derivations are true for any $f(\psi)$ integrable functions. Using a mechanical analogy $f(\psi)$ can be called a *stiffness function*. Substituting it back we find:

$$\ddot{\psi} + f(\psi) + \nu\psi\dot{\psi}^2 = 0 \tag{3.3.3}$$

Let us consider a time instance t_0 and a point in the phase space denoted by $(\psi_0, \dot{\psi}_0)$. Let $\psi(t)$ be a solution of (3.3.1) from these initial conditions, and with choosing another time instance t_1, the point $(\psi_1, \dot{\psi}_1) := (\psi(t_1), \dot{\psi}(t_1))$ is determined.

Let us now integrate (3.3.3) with respect to ψ on the trajectory between these two points. Through the chain rule the integration variable can be changed to time immediately:

$$\int_{\psi_0}^{\psi_1} \left(\ddot{\psi} + f(\psi) + \nu\psi\dot{\psi}^2\right) \mathrm{d}(\psi(t)) = \int_{t_0}^{t_1} \left(\ddot{\psi} + f(\psi) + \nu\psi\dot{\psi}^2\right) \dot{\psi}\mathrm{d}t = 0 \tag{3.3.4}$$

Integration of the first term is straightforward, and the second term leads a simple one-variable integral of the stiffness function:

$$\int_{t_0}^{t_1} \left(\ddot{\psi}\dot{\psi} + f(\psi)\dot{\psi} + \nu\psi\dot{\psi}^3\right) \mathrm{d}t = \left[\frac{1}{2}\dot{\psi}^2\right]_{\dot{\psi}_0}^{\dot{\psi}_1} + \int_{\psi_0}^{\psi_1} f(\psi)\mathrm{d}\psi + \int_{t_0}^{t_1} \nu\psi\dot{\psi}^3\mathrm{d}t \quad (3.3.5)$$

However we cannot find a function depending on ψ and $\dot{\psi}$, from which the third term could be created through a total derivation. That is why the equation could be considered non-integrable in some sense. However its integration can be performed iteratively, using partial integration and (3.3.3) alternately. Let us integrate the third term by parts:

$$\begin{aligned}\int_{t_0}^{t_1} \nu\psi\dot{\psi}^3\mathrm{d}t &= \left[\frac{1}{2}\nu\psi^2\dot{\psi}^2\right]_{t_0}^{t_1} - \int_{t_0}^{t_1} \nu\psi^2\dot{\psi}\ddot{\psi}\mathrm{d}t = \\ &= \left[\frac{1}{2}\nu\psi^2\dot{\psi}^2\right]_{t_0}^{t_1} + \int_{t_0}^{t_1} \nu\psi^2\dot{\psi}\left(f(\psi) + \nu\psi\dot{\psi}^2\right)\mathrm{d}t = \\ &= \left[\frac{1}{2}\nu\psi^2\dot{\psi}^2\right]_{t_0}^{t_1} + \int_{\psi_0}^{\psi_1} (\nu\psi^2)f(\psi)\mathrm{d}\psi + \int_{t_0}^{t_1} (\nu\psi^2)\nu\psi\dot{\psi}^3\mathrm{d}t\end{aligned} \quad (3.3.6)$$

We have to worry only with the last term. Let us apply the same procedure again:

$$\begin{aligned}&\int_{t_0}^{t_1} (\nu\psi^2)\nu\psi\dot{\psi}^3\mathrm{d}t = \\ &\qquad = \left[\frac{1}{4}(\nu\psi^2)^2\dot{\psi}^2\right]_{t_0}^{t_1} + \int_{\psi_0}^{\psi_1} \frac{1}{2}(\nu\psi^2)^2 f(\psi)\mathrm{d}\psi + \int_{t_0}^{t_1} \frac{1}{2}(\nu\psi^2)^2\nu\psi\dot{\psi}^3\mathrm{d}t\end{aligned} \quad (3.3.7)$$

A regularity during these steps can be observable. It can be expressed in the following way:

$$\begin{aligned}&\int_{t_0}^{t_1} \frac{(\nu\psi^2)^k}{k!}\nu\psi\dot{\psi}^3\mathrm{d}t = \\ &\quad = \left[\frac{1}{2}\dot{\psi}^2\frac{(\nu\psi^2)^{k+1}}{(k+1)!}\right]_{t_0}^{t_1} + \int_{\psi_0}^{\psi_1} \frac{(\nu\psi^2)^{k+1}}{(k+1)!}f(\psi)\mathrm{d}\psi + \int_{t_0}^{t_1} \frac{(\nu\psi^2)^{k+1}}{(k+1)!}\nu\psi\dot{\psi}^2\mathrm{d}t\end{aligned} \quad (3.3.8)$$

Repeating this procedure by induction we get the following result:

$$\begin{aligned}&\int_{\psi_0}^{\psi_1} \left(\ddot{\psi} + f(\psi) + \nu\psi\dot{\psi}^2\right)\mathrm{d}\psi(t) = \\ &\qquad = \left[\frac{1}{2}\dot{\psi}^2\sum_{k=0}^{\infty}\frac{(\nu\psi^2)^k}{k!}\right]_{t_0}^{t_1} + \int_{\psi_0}^{\psi_1} f(\psi)\sum_{k=0}^{\infty}\frac{(\nu\psi^2)^k}{k!}\mathrm{d}\psi\end{aligned} \quad (3.3.9)$$

The expression in the summation proves not only convergent, but a simple exponential function:

$$\sum_{k=0}^{\infty} \frac{(\nu\psi^2)^k}{k!} = e^{\nu\psi^2} \tag{3.3.10}$$

Using that we find:

$$\int_{\psi_0}^{\psi_1} \left(\ddot{\psi} + f(\psi) + \nu\psi\dot{\psi}^2\right) \mathrm{d}\psi(t) = \left[\frac{1}{2}\dot{\psi}^2 e^{\nu\psi^2}\right]_{t_0}^{t_1} + \int_{\psi_0}^{\psi_1} f(\psi) e^{\nu\psi^2} \mathrm{d}\psi \tag{3.3.11}$$

Let us define the following function called *potential energy*:

$$U(\psi) := \int_0^{\psi} f(\psi) e^{\nu\psi^2} \mathrm{d}\psi \tag{3.3.12}$$

Using our current $f(\psi)$ from (3.3.2):

$$U(\psi) = \frac{\nu\omega^2 - \mu}{2\nu^2}(e^{\nu\psi^2} - 1) + \psi^2 \frac{\mu}{2\nu} e^{\nu\psi^2} \tag{3.3.13}$$

The integration constant is chosen to have $U(0) = 0$. Similarly an other function called *kinetic energy* can be defined:

$$T(\psi, \dot{\psi}) := \frac{1}{2}\dot{\psi}^2 e^{\nu\psi^2} \tag{3.3.14}$$

Using these functions (3.3.11) can be expressed very briefly:

$$T(\psi_1, \dot{\psi}_1) + U(\psi_1) = T(\psi_0, \dot{\psi}_0) + U(\psi_0) \tag{3.3.15}$$

Let us define the following function:

$$E(\psi, \dot{\psi}) := T(\psi, \dot{\psi}) + U(\psi) \tag{3.3.16}$$

With this (3.3.15) becomes:

$$E(\psi_1, \dot{\psi}_1) = E(\psi_0, \dot{\psi}_0), \tag{3.3.17}$$

that is function E has the same value at points $(\psi_0, \dot{\psi}_0)$ and $(\psi_1, \dot{\psi}_1)$. As the time instance t_1 is chosen arbitrary, the value of E is constant along the trajectory. Therefore E is an energy function of the differential equation, which has a full form of:

$$\boxed{E(\psi, \dot{\psi}) = \frac{1}{2}\dot{\psi}^2 e^{\nu\psi^2} + \frac{1}{2}\frac{\nu\omega^2 - \mu}{\nu^2}(e^{\nu\psi^2} - 1) + \frac{1}{2}\psi^2 \frac{\mu}{\nu} e^{\nu\psi^2}} \tag{3.3.18}$$

The function can be seen in Figure 3.10 for a set of parameters typical to a railway wheelset.

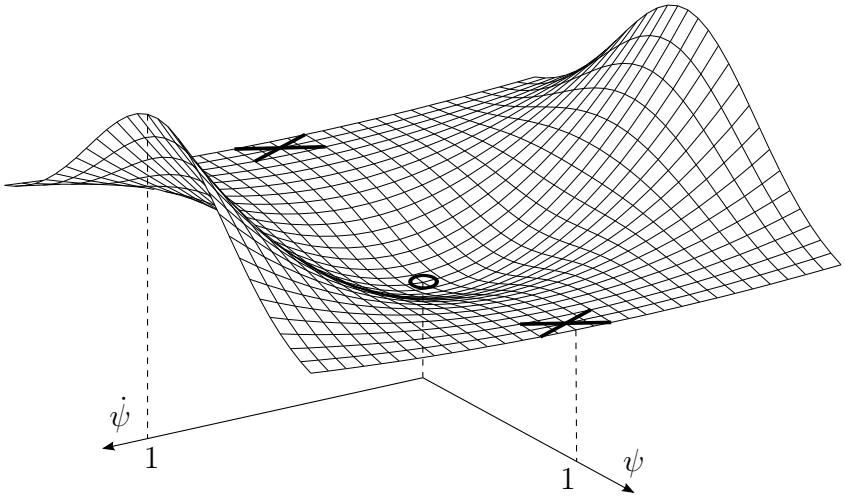

Figure 3.10: Graph of the energy function (3.3.18), $\nu = -3, \mu/\omega^2 = -7/6$. The circle and the two crosses denote the centre and two saddle points, respectively.

This result can be checked if the total derivative of (3.3.18) is calculated:

$$\dot{E} = \frac{\mathrm{d}E}{\mathrm{d}t} = \dot{\psi} e^{\nu\psi^2} \left(\ddot{\psi} + \omega^2 \psi + \mu\psi^3 + \nu\psi\dot{\psi} \right) = 0 \tag{3.3.19}$$

In the brackets we got the differential equation (3.3.1), thus the total derivative of E is identically zero. Moreover, the domain of E covers the whole real plane, therefore (3.3.18) is a global energy function of the system, and (3.3.1) is conservative.

It is interesting, that although a non-potential term $\nu\psi\dot{\psi}^2$ is presented in the equation, the potential and kinetic energy still can be used in the classical sense, and the total energy of the system is obtained by summing the two, similarly as classical conservative systems.

The kinetic energy function simplifies to the usual kinetic energy if $\nu = 0$ is assumed in (3.3.14)

$$T(\psi, \dot{\psi})\Big|_{\nu=0} = \frac{1}{2}\dot{\psi}^2 \tag{3.3.20}$$

It is not trivial that the formula of the potential energy gives back the common result for the Duffing oscillator, as $\nu = 0$ cannot be directly substituted to (3.3.13). However, the limit of it letting $\nu \to 0$ can be calculated:

$$\lim_{\nu \to 0} U(\psi) = \frac{1}{2}\omega^2\psi^2 + \frac{1}{4}\mu\psi^4, \tag{3.3.21}$$

which is the result we expected for the Duffing oscillator.

This procedure can be generalized a bit, if we assume equations in the form:

$$\ddot{\psi} + f(\psi) + g(\psi)\dot{\psi}^2 = 0, \tag{3.3.22}$$

where $g(\psi)$ can be any integrable function. In this case the energy function is:

$$E(\psi,\dot{\psi}) = \frac{1}{2}\dot{\psi}^2 e^{2\int g(\psi)\mathrm{d}\psi} + \int_0^{\psi} f(\psi) e^{2\int g(\psi)\mathrm{d}\psi}\mathrm{d}\psi \tag{3.3.23}$$

If we try to generalize the iteration method having terms $\dot{\psi}^4$ and other higher order even powers of $\dot{\psi}$, it does not work in the way presented before. One should do several iterations embedded to each other and calculations become impracticable.

If the energy function is known, then the trajectories can be calculated as implicit functions. Let us choose a trajectory by picking an $E_0 := E(\psi_0, \dot{\psi}_0)$ value. Then from (3.3.17):

$$\frac{1}{2}\dot{\psi}^2 e^{\nu\psi^2} + \frac{1}{2}\frac{\nu\omega^2-\mu}{\nu^2}(e^{\nu\psi^2}-1) + \frac{1}{2}\psi^2\frac{\mu}{\nu}e^{\nu\psi^2} = E_0 \tag{3.3.24}$$

From this $\dot{\psi}$ can be expressed explicitly:

$$\dot{\psi} = \pm\sqrt{\left(2E_0 + \frac{\nu\omega^2-\mu}{\nu^2}\right)e^{-\nu\psi^2} - \frac{\nu\omega^2-\mu}{\nu^2} - \psi^2\frac{\mu}{\nu}} \tag{3.3.25}$$

Let us denote

$$C := 2E_0 + \frac{\nu\omega^2-\mu}{\nu^2} \tag{3.3.26}$$

Then the equation of the trajectories are:

$$\boxed{\dot{\psi} = \pm\sqrt{Ce^{-\nu\psi^2} - \frac{\nu\omega^2-\mu}{\nu^2} - \psi^2\frac{\mu}{\nu}}} \tag{3.3.27}$$

Some typical trajectories can be seen in Figure 3.11, using the parameter values from Subsection 3.2.4. Similarly to the Duffing oscillator, $\mu < 0$ creates two saddle points at $\psi = \pm\sqrt{\omega^2/\mu}$. If $\mu > 0$, these saddle points are missing and the phase plane is topologically equivalent to the field of a linear centre. The ν parameter does not modify the topology of the phase plane, however it distorts the geometry of it.

3.3.2 General method of finding an energy function

In the last subsection we have found an energy function for the equation, which is in strong analogy with the total mechanical energy. It is obvious that if $E(\psi,\dot{\psi})$ is constant along the curves then any function of E is also constant. In this section the objective is to determine all possible energy functions of the system, and their connection with the (3.3.18) function. The symbols with tilde denotes the general

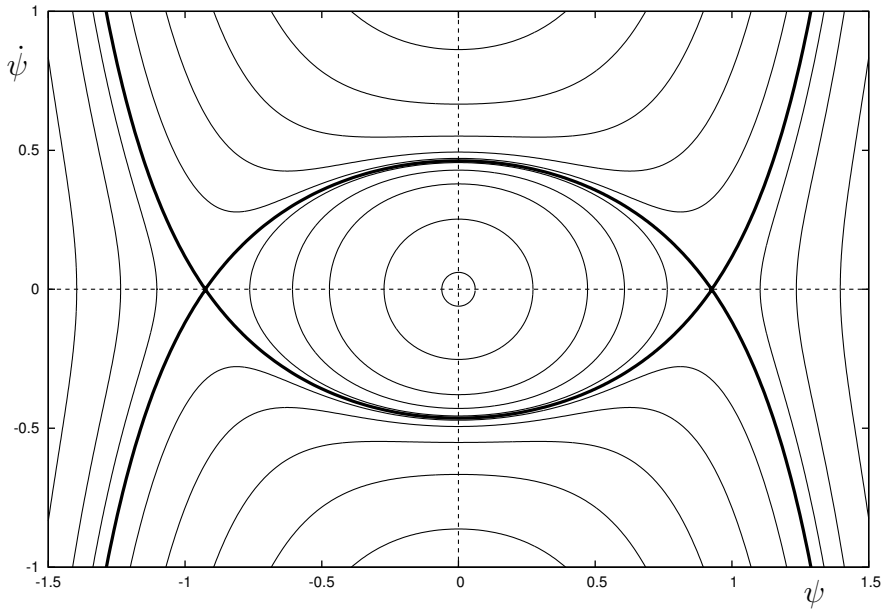

Figure 3.11: Trajectories of the approximated $\psi - \dot{\psi}$ phase plane, $\nu = -3, \mu/\omega^2 = -7/6$. The thick lines denote the heteroclinic orbits of the saddle points.

quantities of this calculation, and plain versions of them refer to the quantities from the previous subsection.

Let us suppose that $\tilde{E}(\psi, \dot{\psi})$ is an energy function of (3.3.1). Then the total derivative of $\tilde{E}$ along the trajectories must be zero:

$$\frac{\mathrm{d}}{\mathrm{d}t}\tilde{E}\left(\psi, \dot{\psi}\right) = \partial_1 \tilde{E}\left(\psi, \dot{\psi}\right)\dot{\psi} + \partial_2 \tilde{E}\left(\psi, \dot{\psi}\right)\ddot{\psi} = 0 \tag{3.3.28}$$

Substituting $\ddot{\psi}$ from the differential equation (3.3.1) we get:

$$\partial_1 \tilde{E}\left(\psi, \dot{\psi}\right)\dot{\psi} - \partial_2 \tilde{E}\left(\psi, \dot{\psi}\right)(\omega^2\psi + \mu\psi^3 + \nu\psi\dot{\psi}^2) = 0 \tag{3.3.29}$$

Let the energy function be analytic, then it can be expanded into Taylor series around the origin. As the trajectories are symmetric respect to the time-reverse symmetry transformations, thus the energy function has to be also symmetric to the ψ and $\dot{\psi}$ axes. This means that the Taylor series can only contain even powers of both variables:

$$\tilde{E}(\psi, \dot{\psi}) = \sum_{i,j=0}^{\infty} \tilde{e}_{ij}\psi^{2i}\dot{\psi}^{2j}, \tag{3.3.30}$$

where the e_{ij} symbols are real numbers to be determined. In fact the whole Taylor series could be used, but the other coefficient later become zero.

Let us write up some terms from the beginning of the series:

$$\tilde{E}(\psi,\dot{\psi}) = e_{00} + e_{10}\psi^2 + e_{01}\dot{\psi}^2 + e_{20}\psi^4 + e_{11}\psi^2\dot{\psi}^2 + e_{02}\dot{\psi}^4 + \mathcal{O}^6(\psi,\dot{\psi}) \tag{3.3.31}$$

After performing the differentiations:

$$\partial_1\tilde{E}(\psi,\dot{\psi}) = 2e_{10}\psi + 4e_{20}\psi^3 + 2e_{11}\psi\dot{\psi}^2 + \mathcal{O}^5(\psi,\dot{\psi}) \tag{3.3.32}$$

$$\partial_2\tilde{E}(\psi,\dot{\psi}) = 2e_{01}\dot{\psi} + 2e_{11}\psi^2\dot{\psi} + 4e_{02}\dot{\psi}^3 + \mathcal{O}^5(\psi,\dot{\psi}) \tag{3.3.33}$$

Now these expressions can be substituted to (3.3.29). After performing the operations a series is obtained, which can be only identically zero if the coefficients of all monomials are zero. It can be checked that only terms being odd in both ψ and $\dot{\psi}$ are present.

The only second-order term we get an equation:

$$\psi\dot{\psi}: \quad 2e_{10} - 2\omega^2 e_{01} = 0 \tag{3.3.34}$$

It can be written into matrix form, which seems not very expedient but helps for recognizing the regularities:

$$[2][e_{10}] = [2\omega^2][e_{01}] \tag{3.3.35}$$

From that the coefficient e_{10} can be expressed with e_{01}, and the energy function can be written into the form:

$$\tilde{E}(\psi,\dot{\psi}) = e_{00} + \left(\omega^2\psi^2 + \dot{\psi}^2\right)e_{01} + \mathcal{O}^4(\psi,\dot{\psi}) \tag{3.3.36}$$

Let us continue with the fourth-order terms, from which two equations can be obtained:

$$\begin{aligned} \psi^3\dot{\psi}: &\quad 4e_{20} - 2e_{01}\mu - 2e_{11}\omega^2 = 0 \\ \psi\dot{\psi}^3: &\quad 2e_{11} - 2e_{01}\nu - 4e_{02}\omega^2 = 0 \end{aligned} \tag{3.3.37}$$

They can be rewritten to matrix form:

$$\begin{bmatrix} 4 & -2\omega^2 \\ 0 & 2 \end{bmatrix}\begin{bmatrix} e_{20} \\ e_{11} \end{bmatrix} = \begin{bmatrix} 2\mu & 0 \\ 2\nu & 4\omega^2 \end{bmatrix}\begin{bmatrix} e_{01} \\ e_{02} \end{bmatrix} \tag{3.3.38}$$

From this the coefficients e_{20} and e_{11} can be determined using e_{01} and e_{02}. With them the energy function can be written as:

$$\begin{aligned} \tilde{E}(\psi,\dot{\psi}) = e_{00} + \left(\omega^2\psi^2 + \dot{\psi}^2 + \nu\psi^2\dot{\psi}^2 + \frac{1}{2}(\mu+\nu\omega^2)\psi^4\right)e_{01} + \\ + \left(\omega^4\psi^4 + 2\omega^2\psi^2\dot{\psi}^2 + \dot{\psi}^4\right)e_{02} + \mathcal{O}^6(\psi,\dot{\psi}) \end{aligned} \tag{3.3.39}$$

This procedure can be continued with the higher-order terms. It can be recognised that each step if we consider the $2k-$th order coefficients from (3.3.29), then k equations can be obtained for the $k+1$ $2k-$th order coefficients of $\tilde{E}$. It can be also proven that these equations are independent, thus in each step all coefficients except one can be determined. If we follow the method above, then for the next j the e_{0j} coefficients can be chosen freely, and the other e_{ij} numbers are determined by the equations.

With having e_{ij} coefficients we have the energy function only if the power series is convergent. Let us assume it now, and examine the convergence later. Let us define the generator function of the energy function:

$$\tilde{G}(y) := \tilde{E}(0, \sqrt{2y}) = \sum_{j=0}^{\infty} \tilde{e}_{0j}(2y)^j = e_{00} + 2e_{01}y + 4e_{02}y^2 + \mathcal{O}^3(y) \tag{3.3.40}$$

It can be recognised, that the right-hand side of the equation is a Taylor series of a general analytic function. Therefore one can choose *any* generator function $\tilde{G}$, and from that an energy function can be determined to fulfil $\tilde{G}\left(\frac{\dot{\psi}^2}{2}\right) = \tilde{E}(0, \dot{\psi})$, if the series is convergent. The resulting $\tilde{E}$ can be written as:

$$\tilde{E}(\psi, \dot{\psi}) = e_{00} + \varepsilon_1(\psi, \dot{\psi})e_{01} + \varepsilon_2(\psi, \dot{\psi})e_{02} + \cdots = e_{00} + \sum_{j=1}^{\infty} \varepsilon_j(\psi, \dot{\psi})e_{0j} \tag{3.3.41}$$

Here the $\varepsilon_j(\psi, \dot{\psi})$ symbols are power series, and can be considered to be functions only if they are convergent at least on a finite region.

For proving that the energy function from the previous subsection can be useful. Let us determine the generator function of (3.3.18):

$$G(y) := E(0, \sqrt{2y}) = y \tag{3.3.42}$$

Comparing it with (3.3.40):

$$\begin{aligned} e_{01} &= \frac{1}{2} \\ e_{0j} &= 0 \quad \text{if} \quad j \neq 1 \end{aligned} \tag{3.3.43}$$

Substituting it to (3.3.41):

$$E(\psi, \dot{\psi}) = \frac{1}{2}\varepsilon_1(\psi, \dot{\psi}) \tag{3.3.44}$$

From that:

$$\varepsilon_1(\psi, \dot{\psi}) = 2E(\psi, \dot{\psi}), \tag{3.3.45}$$

thus $\varepsilon_1(\psi, \dot{\psi})$ has to be convergent and it is proportional to E. This fact can be illustrated by expanding (3.3.18) to Taylor series:

$$E(\psi, \dot{\psi}) = \frac{1}{2}\left(\omega^2\psi^2 + y^2 + \nu\psi^2 y^2 + \frac{1}{2}(\mu + \nu\omega^2)\right) + \mathcal{O}^6(\psi, \dot{\psi}) \tag{3.3.46}$$

Comparing with (3.3.39) the identity up to the fourth order terms can be checked.

This method can be applied to all $\varepsilon_k(\psi, \dot{\psi})$ functions having

$$G_k(y) := E^k(0, \sqrt{2y}) \tag{3.3.47}$$

From that, similarly as above we find:

$$\varepsilon_k(\psi, \dot{\psi}) = (2E)^k(\psi, \dot{\psi}) \tag{3.3.48}$$

With this, (3.3.41) becomes:

$$\tilde{E}(\psi, \dot{\psi}) = e_{00} + \sum_{j=1}^{\infty} e_{0j}(2E)^j(\psi, \dot{\psi}) = (\tilde{G} \circ E)(\psi, \dot{\psi}) \tag{3.3.49}$$

Therefore any energy function of equation (3.3.1) can be written in the form:

$$\boxed{\tilde{E}(\psi, \dot{\psi}) = (\tilde{G} \circ E)(\psi, \dot{\psi}),} \tag{3.3.50}$$

where $E(\psi, \dot{\psi})$ is the function determined in (3.3.18) and $\tilde{G}$ is an arbitrary analytic function.

From this result the new information is clearly not the trivial fact that a function of the conserved quantity E is also conserved, but the fact that all conserved quantity is the function of E. Moreover, the iterative method in the previous subsection produces the simplest relevant energy function provided by the general method.

3.3.3 Hamiltonian and Lagrangian formulation

If only the second-order differential equation is known, usually is not easy to reconstruct the Hamiltonian and Lagrangian functions from which the equation can be derived. But as our system in (3.3.1) has proved conservative and the energy function is derived in (3.3.18), this calculations can be done systematically.

Let us assume, that the Hamiltonian can be written in the form $H(\psi, p)$, where p is the general momentum corresponding to ψ. The assumption that the explicit time-dependence is not present in H, could be obtained using Noether's Theorem,

but it is also reasonable from the analogy with one degree-of-freedom conservative mechanical systems.

The Hamiltonian equations generated by $H(\psi, p)$ are:

$$\begin{aligned} \dot{\psi} &= \partial_2 H(\psi, p) \\ \dot{p} &= -\partial_1 H(\psi, p) \end{aligned} \tag{3.3.51}$$

We can consider this system equivalent to equation (3.3.18), if performing an appropriate $p(\psi, \dot{\psi})$ substitution, the two systems give the same solutions for ψ.

It can be checked using the Hamilton equations, that the total derivative of H is zero:

$$\dot{H} = \dot{\psi}\partial_1 H + \dot{p}\partial_2 H = -\dot{\psi}\dot{p} + \dot{p}\dot{\psi} = 0, \tag{3.3.52}$$

that is H is a conserved quantity. It is known that every conserved quantity has to be in the form (3.3.50), thus

$$H \circ p = \tilde{E} = \tilde{G} \circ E \tag{3.3.53}$$

for any ψ, $\dot{\psi}$. Let us differentiate both sides of (3.3.53) partially respect to ψ and $\dot{\psi}$:

$$\begin{aligned} \partial_1 H \circ p + (\partial_2 H \circ p)\partial_1 p &= (\partial \tilde{G} \circ E)\partial_1 E \\ (\partial_2 H \circ p)\partial_2 p &= (\partial \tilde{G} \circ E)\partial_2 E \end{aligned} \tag{3.3.54}$$

Let us substitute the derivatives of H from (3.3.51):

$$\begin{aligned} -\dot{p} + \dot{\psi}\partial_1 p &= (\partial \tilde{G} \circ E)\partial_1 E \\ \dot{\psi}\partial_2 p &= (\partial \tilde{G} \circ E)\partial_2 E \end{aligned} \tag{3.3.55}$$

The total derivative of p is:

$$\dot{p} = \dot{\psi}\partial_1 p + \ddot{\psi}\partial_2 p \tag{3.3.56}$$

Substituting it to (3.3.55):

$$\begin{aligned} -\ddot{\psi}\partial_2 p &= (\partial \tilde{G} \circ E)\partial_1 E \\ \dot{\psi}\partial_2 p &= (\partial \tilde{G} \circ E)\partial_2 E \end{aligned} \tag{3.3.57}$$

Calculating the second equation of (3.3.57):

$$\partial_2 p = \frac{(\partial \tilde{G} \circ E)\partial_2 E}{\dot{\psi}} \tag{3.3.58}$$

Substituting it back to the first equation of (3.3.57):

$$\dot{\psi}(\partial\tilde{G}\circ E)\partial_1 E + \ddot{\psi}(\partial\tilde{G}\circ E)\partial_2 E = 0 \tag{3.3.59}$$

$$(\partial\tilde{G}\circ E)\dot{E} = 0 \tag{3.3.60}$$

The last equality stands identically because E is an energy function.

The conclusion is that the only restriction to p is from (3.3.58):

$$\partial_2 p = \frac{(\partial\tilde{G}\circ E)\dot{\psi}e^{\nu\psi^2}}{\dot{\psi}} \tag{3.3.61}$$

Thus the possible p functions are:

$$p(\psi,\dot{\psi}) = \int \frac{(\partial\tilde{G}\circ E)\dot{\psi}e^{\nu\psi^2}}{\dot{\psi}}\mathrm{d}\dot{\psi} + h(\psi), \tag{3.3.62}$$

where h is an arbitrary function. We can choose the generator function $\tilde{G}$ and h freely, but the simplest case is preferred, when $h(\psi) = 0$ and $\tilde{G}$ is the identity mapping. Then:

$$\boxed{p(\psi,\dot{\psi}) = \dot{\psi}e^{\nu\psi^2}} \tag{3.3.63}$$

Choosing $\tilde{G}$ identity makes (3.3.53):

$$H\circ p = E \tag{3.3.64}$$

Therefore the inverse of p is needed to determine the Hamiltonian:

$$\dot{\psi} = p(\psi,\dot{\psi})e^{-\nu\psi^2} \tag{3.3.65}$$

Finally, the Hamiltonian is:

$$H(\psi,p) = E(\psi,\dot{\psi})\Big|_{\dot{\psi}=pe^{-\nu\psi^2}} \tag{3.3.66}$$

After substitution we get:

$$\boxed{H(\psi,p) = \frac{1}{2}p^2e^{-\nu\psi^2} + \frac{1}{2}\frac{\nu\omega^2-\mu}{\nu^2}(e^{\nu\psi^2}-1) + \frac{1}{2}\psi^2\frac{\mu}{2\nu}e^{\nu\psi^2}} \tag{3.3.67}$$

From that the Hamiltonian equations are:

$$\begin{aligned}\dot{p} &= \nu\psi p^2e^{-\nu\psi^2} - \omega^2\psi e^{\nu\psi^2} - \mu\psi^3e^{\nu\psi^2}\\ \dot{\psi} &= pe^{-\nu\psi^2}\end{aligned} \tag{3.3.68}$$

Having the Hamiltonian it becomes straightforward to calculate the Lagrangian by definition:

$$L(\psi,\dot{\psi}) := p(\psi,\dot{\psi})\dot{\psi} - H(\psi,p(\psi,\dot{\psi})) = p(\psi,\dot{\psi})\dot{\psi} - E(\psi,\dot{\psi}) \tag{3.3.69}$$

$$\boxed{L(\psi,\dot{\psi}) = \frac{1}{2}\dot{\psi}^2 e^{\nu\psi^2} - \frac{1}{2}\frac{\nu\omega^2-\mu}{\nu^2}(e^{\nu\psi^2}-1) - \frac{1}{2}\psi^2\frac{\mu}{2\nu}e^{\nu\psi^2}} \tag{3.3.70}$$

From that the Lagrange equations can be used:

$$\frac{\mathrm{d}}{\mathrm{d}t}\partial_2 L(\psi,\dot{\psi}) - \partial_1 L(\psi,\dot{\psi}) = 0, \tag{3.3.71}$$

and the equation we obtain is:

$$e^{\nu\psi^2}\left(\ddot{\psi} + \omega^2\psi + \mu\psi^3 + \nu\psi\dot{\psi}\right) = 0, \tag{3.3.72}$$

which is equivalent to our differential equation (3.3.1).

It is interesting, that the Lagrange function can be calculated as the difference of the kinetic and potential energy defined in the last subsection:

$$L(\psi,\dot{\psi}) = T(\psi,\dot{\psi}) - U(\psi) \tag{3.3.73}$$

This fact arises from the analogy to simple mechanical systems. The connection between the general momentum p and the kinetic energy T is also the same as in mechanics:

$$T(\psi,\dot{\psi}) = \frac{1}{2}p(\psi,\dot{\psi})\dot{\psi} \tag{3.3.74}$$

3.3.4 Approximate solution around the origin

In (3.3.27) the trajectories has been determined, but we do not know much about the solution of (3.3.1) along the time. The exact analytical solution seems to be a dream, because it does not exist already for the equation for the Duffing oscillator. But there are possibilities to include the effect of the nonlinear terms of μ and ν into approximate solutions.

One well-known method is called the small-parameter perturbation method which was developed first by Poincare. The method starts from the linear equation and the nonlinear solution is created through a series of functions using the nonlinear parameters for a Taylor expansion. The method is used for the Duffing oscillator in the book of Malkin [14], now the same formulation is applied for (3.3.1). The main difference comes from the two-variable expansion and the handling of the $\dot{\psi}$ term.

It is derived in Subsection 3.1.4, that there is a neighbourhood around the origin where all trajectories are closed. From (3.3.27) this range could be calculated explicitly, but this is not very important now. If an orbit is closed and contains the origin, it must intersect both axes. Therefore one can investigate the solution of the following initial condition problem without the loss of generality:

$$\begin{aligned} \ddot{\psi} + \omega^2\psi + \mu\psi^3 + \nu\psi\dot{\psi}^2 = 0 \\ \psi(0) = A \\ \dot{\psi}(0) = 0 \end{aligned} \tag{3.3.75}$$

A is a positive real number and can be called to the amplitude of the solution.

It is useful to rescale the variable with A and the time with ω:

$$y(t) := \frac{\psi(t/\omega)}{A} \tag{3.3.76}$$

Two new parameters are also introduced:

$$\lambda_1 := \frac{A^2\mu}{\omega^2} \tag{3.3.77}$$

$$\lambda_2 := A^2\nu \tag{3.3.78}$$

With this substitutions (3.3.75) becomes:

$$\begin{aligned} \ddot{y} + y + \lambda_1 y^3 + \lambda_2 y\dot{y}^2 = 0 \\ y(0) = 1 \\ \dot{y}(0) = 0 \end{aligned} \tag{3.3.79}$$

Let us suppose that with this initial condition the curve of the solution is in the periodic region. Let T be the time period of the solution, that is:

$$y(t+T) = y(t) \tag{3.3.80}$$

Then the angular frequency of the solution can be calculated:

$$\beta := \frac{2\pi}{T} \tag{3.3.81}$$

This quantity depends on the parameters λ_1 and λ_2. Let us suppose that the square of β can be written as a Taylor series of these parameters:

$$\beta^2(\lambda_1, \lambda_2) = \sum_{i,j=0}^{\infty} g_{ij}\lambda_1^i\lambda_2^j, \tag{3.3.82}$$

where g_{ij} mean real coefficients. The expansion is done around $\lambda_1 = \lambda_2 = 0$,that is why they are called the *small parameters*. Let us note that not μ or ν themselves are considered to be small, but their product with the square of the amplitude A of the solution. If we check the simplest case, $\lambda_1 = \lambda_2 = 0$, from the solution of the linear equation we get:

$$\beta^2(0,0) = g_{00} = 1 \tag{3.3.83}$$

The main idea of Poincare's method to expand the solution $y(t)$ to a Taylor series of functions using again the small parameters λ_1 and λ_2:

$$y(t) = \sum_{i,j=0}^{\infty} y_{ij}(t)\lambda_1^i\lambda_2^j \tag{3.3.84}$$

The functions y_{ij} are supposed to be all T-periodic:

$$y_{ij}(t+T) = y_{ij}(t) \tag{3.3.85}$$

From the point of view of the initial conditions, the leading term y_{00} is considered to be different from the other ones. The leading term has to fulfil the initial conditions of (3.3.79).

$$\begin{aligned} y_{00}(0) &= 1 \\ \dot{y}_{00}(0) &= 0 \end{aligned} \tag{3.3.86}$$

However the other $y_{ij} \neq y_{00}$ terms all have homogeneous initial conditions:

$$\begin{aligned} y_{ij}(0) &= 0 \\ \dot{y}_{ij}(0) &= 0 \end{aligned} \tag{3.3.87}$$

This is a usual method used at perturbation calculations, and makes any finite slice of the function series exactly compatible to the initial conditions. Moreover one have not to worry about the convergence of the functions at the initial time instance. The y_{ij} terms are considered to be corrections superposed to the leading approximation y_{00}. It is very important to see, that y_{00} is not the solution of the linear equation, because it has an angular frequency β but not 1. Although β is not known, the terms of the series of β and $y(t)$ are determined simultaneously during the calculations.

Let us substitute the series of $y(t)$ to the differential equations. For making easier to follow the calculations, only the first few terms of the series are written:

$$\begin{aligned} &(\ddot{y}_{00} + \lambda_1\ddot{y}_{10} + \lambda_2\ddot{y}_{01} + \dots) + \\ &(y_{00} + \lambda_1 y_{10} + \lambda_2 y_{01} + \dots) + \lambda_1(y_{00} + \lambda_1 y_{10} + \lambda_2 y_{01} + \dots)^3 + \\ &+\lambda_2(y_{00} + \lambda_1 y_{10} + \lambda_2 y_{01} + \dots)(\dot{y}_{00} + \lambda_1\dot{y}_{10} + \lambda_2\dot{y}_{01} + \dots)^2 = 0 \end{aligned} \tag{3.3.88}$$

As we want to obtain solutions of angular frequency β, the ‚1' multiplier of the linear term is expressed from (3.3.82). The last term is also multiplied by a fraction ‚β^2/β^2', but expressed with (3.3.82) in the numerator. These are important to cancel out later the β^2 multipliers arise from the derivation of the solution:

$$\begin{aligned}(\ddot{y}_{00}+\lambda_1\ddot{y}_{10}+\lambda_2\ddot{y}_{01}+\dots)+(\beta^2-\lambda_1 g_{10}-\lambda_2 g_{01}-\dots)\cdot\\ \cdot(y_{00}+\lambda_1 y_{10}+\lambda_2 y_{01}+\dots)+\lambda_1(y_{00}+\lambda_1 y_{10}+\lambda_2 y_{01}+\dots)^3+\\ +\lambda_2(y_{00}+\lambda_1 y_{10}+\lambda_2 y_{01}+\dots)\cdot\frac{1+\lambda_1 g_{10}+\lambda_2 g_{01}+\dots}{\beta^2}\cdot\\ \cdot(\dot{y}_{00}+\lambda_1\dot{y}_{10}+\lambda_2\dot{y}_{01}+\dots)^2=0\end{aligned} \tag{3.3.89}$$

Now the terms according to the different powers of the small parameters are collected. In the first step the ‚constant' terms are considered, which not contain the small parameters:

$$\lambda_1^0\lambda_2^0: \quad :\ddot{y}_{00}+\beta^2 y_{00}=0 \tag{3.3.90}$$

From this simple linear equation the leading solution can be calculated using the initial conditions from (3.3.86):

$$y_{00}(t)=\cos(\beta t) \tag{3.3.91}$$

Now the terms being first-order in λ_1 are examined:

$$\lambda_1^1\lambda_2^0: \quad :\ddot{y}_{10}+\beta^2 y_{10}-g_{10}y_{00}+y_{00}^3=0 \tag{3.3.92}$$

Substituting (3.3.91) and rearranging:

$$\ddot{y}_{10}+\beta^2 y_{10}=g_{10}\cos(\beta t)+\cos^3(\beta t) \tag{3.3.93}$$

Let us perform the Fourier-expansion on the right-hand side of the equation to get rid of the $\cos^3$ term:

$$\ddot{y}_{10}+\beta^2 y_{10}=\left(g_{10}-\frac{3}{4}\right)\cos(\beta t)-\frac{1}{4}\cos(3\beta t) \tag{3.3.94}$$

This is a linear inhomogeneous equation for y_{10}. The homogeneous solution has an angular frequency of β. Therefore the $\cos(\beta)$ terms in the excitation cause resonant solution of the equation. As all y_{ij} functions in the series is supposed to be periodic according to (3.3.85), the coefficient of the potential resonant excitation term must be zero:

$$g_{10}=\frac{3}{4} \tag{3.3.95}$$

After that condition (3.3.94) can be solved using the initial conditions (3.3.87):

$$y_{10} = \frac{1}{32\beta^2}\left(\cos(3\beta t) - \cos(\beta t)\right) \tag{3.3.96}$$

The terms linear in λ_2 are examined in the similar way:

$$\lambda_1^0\lambda_2^1: \quad : \ddot{y}_{01} + \beta^2 y_{01} - g_{01}y_{00} + \frac{1}{\beta^2}y_{00}\dot{y}_{00}^2 = 0 \tag{3.3.97}$$

Substituting the known y_{00} function we get:

$$\ddot{y}_{01} + \beta^2 y_{01} = g_{01}\cos(\beta t) + \sin^2(\beta t)\cos(\beta t) \tag{3.3.98}$$

The β^2 term is cancelled because during the derivation of $\dot{y}_{00}^2$ a β^2 multiplier appears. It can be shown for the higher order steps, that any even function being in Fourier series of leading angular frequency β cause the same cancellation. Let us transform the right-hand side similarly as before:

$$\ddot{y}_{01} + \beta^2 y_{01} = \left(g_{01} - \frac{1}{4}\right)\cos(\beta t) + \frac{1}{4}\cos(3\beta t) \tag{3.3.99}$$

This is a linear differential equation for y_{01}. Avoiding the resonance explained above, the coefficient of $\cos(\beta t)$ is prescribed to be zero:

$$g_{01} = \frac{1}{4} \tag{3.3.100}$$

Solving (3.3.99):

$$y_{01} = -\frac{1}{32\beta^2}\left(\cos(3\beta t) - \cos(\beta t)\right) \tag{3.3.101}$$

Let us summarize the results after calculating the first-order terms. The square of the angular frequency β is in linear approximation:

$$\beta^2 = 1 + \frac{3}{4}\lambda_1 + \frac{1}{4}\lambda_2 + \mathcal{O}^2(\lambda_1, \lambda_2) \tag{3.3.102}$$

Also the first nonlinear approximation of the solution can be determined:

$$y(t) = \cos(\beta t) + \frac{1}{32\beta^2}(\lambda_1 - \lambda_2)\left(\cos(3\beta t) - \cos(\beta t)\right) + \mathcal{O}^2(\lambda_1, \lambda_2) \tag{3.3.103}$$

Now the method is not continued towards the higher-order terms but it can be done formally, this can be checked if we examine the structure of the steps made before. In each step a homogeneous linear equation with β^2 angular frequency is to be solved, and the excitation can be calculated from the known lower-order solutions. To avoiding the resonance an equation can be expressed to determine

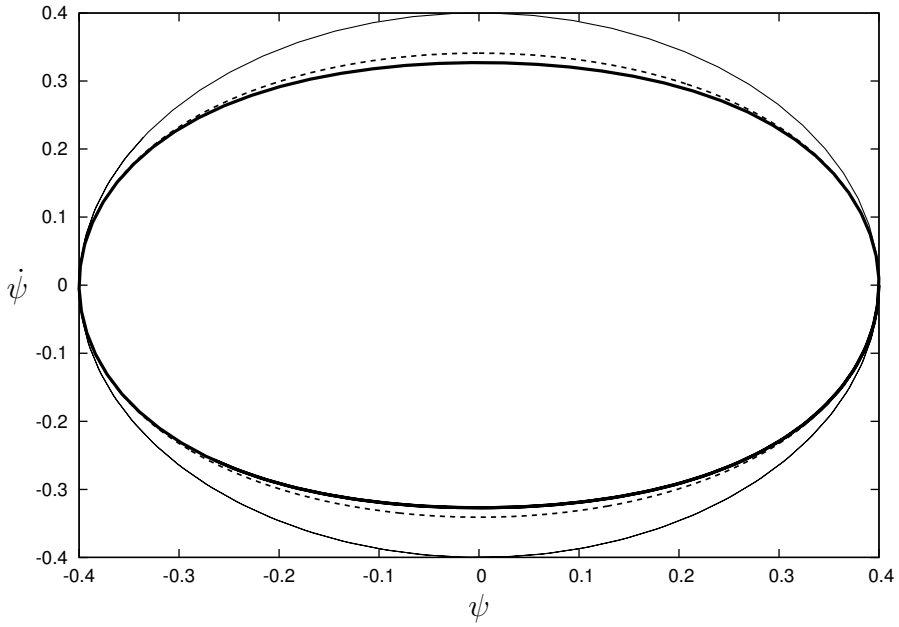

Figure 3.12: Trajectories from the perturbation method, $\omega = 1, \nu = -3, \mu/\omega^2 = -7/6, A = 0.4$. The thick continuous line denotes the first nonlinear approximation according to (3.3.106), while the thin line corresponds to the trajectory from the linear equation. The dashed line is the analytic trajectory from (3.3.27).

a new g_{ij} coefficient for the series of β^2 and after the new $y_{ij}(t)$ solution can be calculated.

However one should be worried about the convergence of these series both for β^2 and $y(t)$. The convergence of the method is proven for the $\nu = 0$ equation in [14], but presence of the derivative of the functions might cause problems about it. The convergence of the method for the equation (3.3.1) remains an open question in this derivation.

Anyway, if the orbits are close to the origin, that is, A is small, then the small parameters are much smaller than one, and already the first-order correction of the frequency and of the solution can be used. Let us transform the solutions back to the original variables and parameters. Then the nonlinear angular frequency is approximately (β now corresponds to the original time variable):

$$\frac{\beta^2}{\omega^2} \approx 1 + A^2 \frac{3\mu + \nu\omega^2}{4\omega^2} \tag{3.3.104}$$

$$\boxed{\beta \approx \omega \sqrt{1 + A^2 \frac{3\mu + \nu\omega^2}{4\omega^2}}} \tag{3.3.105}$$

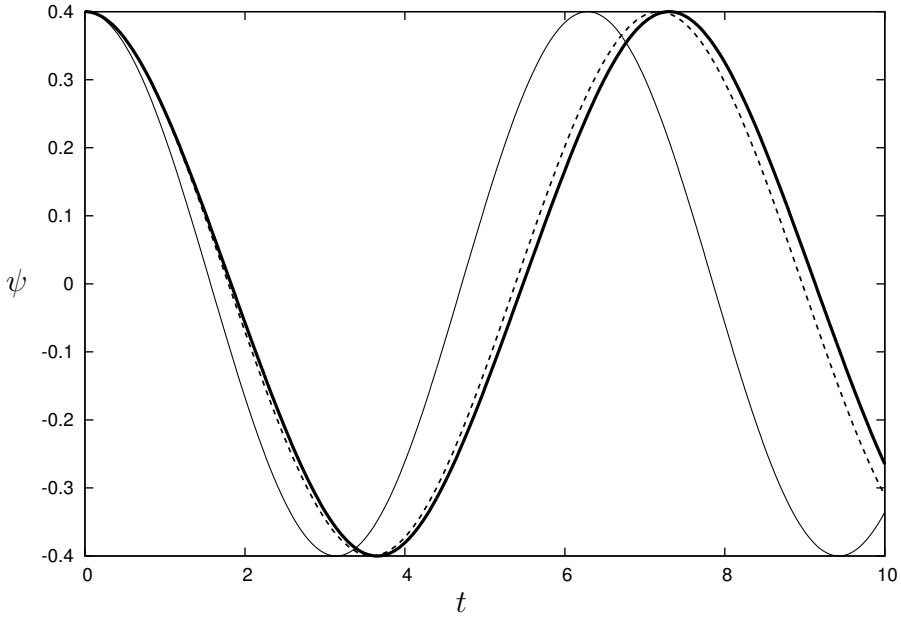

Figure 3.13: Time diagram of ψ from perturbation method, $\omega = 1, \nu = -3, \mu/\omega^2 = -7/6, A = 0.4$. Meaning of the continuous lines is the same as in Figure 3.12. The dashed line corresponds to numerical simulation of (3.3.1) using fourth-order Runge-Kutta method.

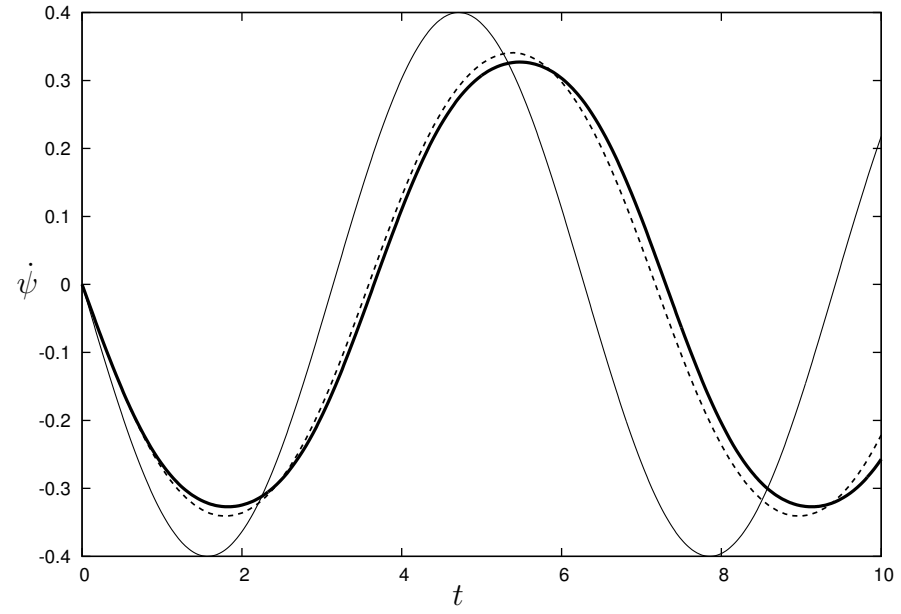

Figure 3.14: Time diagram of $\dot{\psi}$ from perturbation method, $\omega = 1, \nu = -3, \mu/\omega^2 = -7/6, A = 0.4$. Meaning of the continuous lines is the same as in Figure 3.12. The dashed line corresponds to numerical simulation of (3.3.1) using fourth-order Runge-Kutta method.

Also the solution for $\psi(t)$ can be given approximately:

$$\boxed{\psi(t) \approx A\cos(\beta t) + A^3 \frac{\mu - \nu\omega^2}{32\beta^2}\left(\cos(3\beta t) - \cos(\beta t)\right)} \tag{3.3.106}$$

For the first sight the parameter ν does not mean qualitatively new behaviour in the approximate solution compared to μ. However it can be observed, that in that approximation using a positive μ and ν cause the same effect on the frequency, the positiveness of these parameters increase the β angular frequency.

But considering the approximate solution the two parameters have opposite effect, the positive values of μ and ν mean an opposite perturbation in the terms $\cos(3\beta t) - \cos(\beta t)$. The expression $\mu - \nu\omega^2$ in (3.3.106) has appeared already in the expression of the trajectories in (3.3.27).

A similar perturbation method can be found in the textbook of Jordan and Smith [8] (page 138), and if we apply it for our equation, the result are not the same, but they coincide for the linear terms of the small parameters.

If we choose the typical values of the parameters from Subsection 3.2.4, we obtain:

$$\beta \approx \omega\sqrt{1 - A^2\frac{13}{8}}, \tag{3.3.107}$$

which means that the angular frequency is decreased by the nonlinear effects. The trajectories for these parameters can be seen in Figure 3.12, the time diagrams of the approximation can be found in Figures 3.13-3.14 compared with analytic and numeric results. It can be seen that the nonlinear approximation provides a large improvement in accuracy compared to the linear model.

Conclusion

Our mechanical model included simple assumptions but derivation of the nonlinear equation of motion is not trivial at many points of the calculation. It turned out, that this system has four degrees of freedom in the geometric point of view, from which two coordinates describe the natural motion and the other two correspond to the hunting motion. The kinematic constraints reduce the degrees of freedom to zero in the point of view of velocities, they provide the equations of motion without Newton's Second Law, in fact the models lead to a problem of pure kinematics.

Coordinates of the natural motion prove cyclic, therefore the dynamics of the system is determined by only the restricted system two other variables. Natural motion of the whole system corresponds to the origin in this two-dimensional system. This fixed point is neutrally stable in linear approximation, and from the symmetric properties of the system the neutral stability of the nonlinear system can be also proven. Therefore solutions of small perturbations around the natural motion are periodic independently from the velocity. That is, there is not a critical speed in the one-point rolling model, the system is on the boundary of stability at any velocity. Hence stability problems of the hunting have to arise purely from the creep effect, which is caused physically by slip and deformation.

After transforming the time variable the equations of the restricted system can be reformulated as a single second-order differential equation which results a strong analogy with one degree-of-freedom mechanical systems. This analogy can be exploited during the third-order approximation of the equation, the energy function can be derived and the problem can be expressed as a Hamiltonian or Lagrangian system. Using perturbation methods the approximations of the periodic solutions and the nonlinear angular frequency can be determined, on which effects of nonlinearities can be observed.

Many aspect of this model could be explored in the future. For example, different boundary conditions for the connection between the vehicle and the wheelset

can be used. If we chose pulling with a constant force instead of a constant velocity, then a five-dimensional system could be obtained, which would obtain already a Newtonian equations. More complicated models of the bearings could be used with springs and dampers.

An other direction of improvement is to calculate the contact forces and examine the conditions of sliding at the case of one-point rolling with a friction model. Sliding can occur at both contact points at the same time, but geometry allows the wheelset to slide at one of the contact points and roll at the other one. From this simple assumption a critical speed might be obtained. The whole problem could be examined on a curved track, which brakes one of the symmetries of the system and may cause interesting effects.

Probably the most important question that is it whether possible to combine the nonlinear rigid motion with the advanced contact mechanics models with creep. Maybe it is possible, but we should judge if it is worth from practical point of view, which could be decided by a quantitative comparison of the effects of three-dimensional motion and creep.

Since I started working on this project, I usually watch wheels of the trains more carefully. Technical complications like hunting motion always remind me that our technical creations and scientific theories are always imperfect. Hence although we are continuously trying to make them better, it is useful to see, that technical development cannot fulfil the deep desire of perfection in the hearts of human beings. Because the One, who entrusted us to 'conquer the world', said also that 'set your hearts on the kingdom of the Father *first*'.

O veritas Deus: fac me unum tecum in caritate perpetua. Taedet me saepe multa legere et audire: in te est totum, quod volo et desidero. Miserere mei secundum misericordiam tuam.

List of Figures

Summary

In this diploma thesis the so-called hunting motion is investigated, which occurs at the dynamics of railway wheelsets. Hunting is a vibration of three-dimensional motion of the wheelset, which is caused by its concial shape, and which has usually unpleasant consequences in the practice.

After summarizing the phenomenon and the existing models we create a mechanical model to analyse the three-dimensional motion of the wheelset. A single wheelset is considered which is towed on a straight track with a constant velocity. Both the wheelset and the rails are assumed to be rigid, with a one-point contact and pure rolling between them.

The equation of motion is derived by following the positions of the contact points during applying the constraints on the system. During the calculations there is no linearisation, therefore the equations remain relevant also for large values of the parameters and the variables. Dynamics of the system is examined on the equation of motion, the singularities and fixed points are determined. We investigate stability of the natural – free from hunting – motion of the wheelset by linear and nonlinear methods.

Due to the type and amount of constrains this model does not result a real equation of motion in the classical mechanical sense, but the equations can be transformed to a second-order differential equation which can be examined by the usual methods of mechanics. We try to find conserved quantities and the system is expressed by Lagrangian and Hamiltonian formulations. We investigate the nonlinear approximate solutions for small values of perturbations in the initial condition. The model can be improved in the future at several points, finally we introduce the possible directions about that.

Összefoglalás

A diplomamunkában az úgynevezett *vadászó mozgás* jelenségével foglalkozunk, mely a vasúti kerekek dinamikájánál fordul elõ. A vadászó mozgás a kerekek három dimenziós mozgásában megjelenõ rezgés, melyet a kerekek kúpos alakja idéz elõ, és mely gyakorlati szempontból általában kedvezõtlen.

A jelenség és a használatos modellek áttekintése után egy mechanikai modellt hozunk létre, mely képes a kerék három dimenziós mozgásának leírására. Egy egyszerû kerék-párt tekintünk, melyet állandó sebességgel vontatnak egy egyenes vágányon. Mind a kerék-párt, mind a síneket merev testnek feltételezzük, melyek között egy-pontos kapcsolat és tiszta gördülés van.

A mozgásegyenlet levezetését a kényszerek felírása közben az érintési pontok helyzetének követésével végezzük. A levezetés során nem linearizálunk, így a kapott egyenletek érvényesek lesznek a paraméterek és változók nagy értékei esetén is. A rendszer dinamikáját a mozgásegyenletek segítségével vizsgáljuk és meghatározzuk az egyensúlyi helyzeteket és szinguláris pontokat. A természetes – vadászó mozgástól mentes – mozgás stabilitását lineáris és nemlineáris módszerekkel is elemezzük.

A kényszerek jellege és száma miatt a modell nem eredményez valódi mozgásegyenletet a klasszikus mechanikai értelemben, de az egyenletek másodrendû differenciálegyenletté alakíthatók, mely már vizsgálható a mechanika megszokott módszereivel. Igyekszünk megmaradó mennyiséget találni és a rendszert Lagrange- valamint Hamilton-egyenletek segítségével is jellemezzük. A kezdeti értékekben fellépõ kis zavarások esetén vizsgáljuk a megoldásokat nemlineáris közelítés segítségével. A modell a jövõben számos ponton továbbfejleszthetõ, végezetül ennek lehetséges irányait tekintjük át.

Bibliography

[1] Carter, F. W. On the action of a locomotive driving wheel. *Proc. Royal Society 112* (1926), 151–157.

[2] Gantmacher, F. *Lectures in Analytical Mechanics*. MIR Publishers, 1975.

[3] Hertz, H. Ueber die berührung fester elastischer körper. *Journal f. d. reine u. angewandte Mathematik 92* (1882), 156–171.

[4] Holzapfel, G. A. *Nonlinear Solid Mechanics*. John Wiley and Sons, 2000.

[5] Iwnicki, S., Ed. *Handbook of Railway Vehicle Dynamics*. CRC Press, 2006.

[6] Johnson, K. L. A shakedown limit in rolling contact. In *ASME: Proceedings of the Fourth National Congress of Applied Mechanics* (1962), pp. 971–975.

[7] Johnson, K. L. *Contact Mechanics*. Cambridge University Press, 1985.

[8] Jordan, D. W., and Smith, P. *Nonlinear Ordinary Differential Equations*, fourth ed. Oxford University Press, 2007.

[9] Kalker, J. J. *On the Rolling Contact of Two Elastic Bodies in the Presence of Dry Friction*. PhD thesis, Delft University of Technology, 1967.

[10] Kalker, J. J. *Three-Dimensional Elastic Bodies in Rolling Contact*. Kluwer Academic Publishers, Dordrecht, 1990.

[11] Klingel, J. Ueber den lauf von eisenbahnwagen auf gerader bahn. *Organ für die Fortschritte des Eisenbahnwesens 20* (1883).

[12] Knothe, K. History of wheel/rail contact mechanics: from Redtenbacher to Kalker. *Vehicle System Dynamics 46* (2008), 9–26.

[13] Lorant, G. Vasúti kerekek gördülésének dinamikája. diploma thesis, Budapest University of Technology and Economics, 1993.

[14] Malkin, I. G. *Theory of stability of motion (in Russian).* State Publishing House of Technical-Theoretical Literature, Moscow, 1952.

[15] Reynolds, O. On rolling friction. *Phil. Trans. Royal Society 166* (1875), 155.

[16] Strogatz, S. H. *Nonlinear Dynamics and Chaos.* Perseus Books, 1994.

[17] Wickens, A. H. *Fundamentals of Rail Vehicle Dynamics : Guidance and Stability.* Swets and Zeitlinger, Lisse, 2003.

[18] Wiggins, S. *Introduction to Applied Nonlinear Dynamical Systems and Chaos*, 2nd ed. Springer, 2003.